AUTHOR'S RESPONSE **Manuscript acp-2019-1078**

The authors thank the reviewers for their valuable comments, which were very helpful in improving the presentation of the oxidative flow reactor conditions, clarity of the structure, and the overall precision of the manuscript. In the following response to the review, we provide point-by-point responses to the questions posed by the reviewers. The replies to the comments are indicated as red text. After the answers to the referee comments, the revised manuscript text with changes visible is provided, including the modifications to tables and figures.

Anonymous Referee #1

GENERAL COMMENTS:

This article adresses photochemical aging of residential wood combustion (RWC) emission from two stoves at the home-built PEAR oxidatation flow reactor, reaching OH exposures representative of aging of up to one week in the atmosphere. This is one of few studies adressing the topic of RWC aging in OFRs with a suite of state-of-the art mass spectrometric online and offline techniques and adds value for the scientific community.

In my view, the manuscript is of high scientific quality and presents relevant results from a comprehensive study. The language and structure, however, lack clarity and some information is redundant which makes the manuscript unnecessarily long and the core findings quite dilute. I suggest that this be improved to make the article more concise and easier to follow and understand for the readers. I believe this is feasible with major revisions of text and paragraph structure in order to allow more clarity on the main findings, conclusions and limitations of the study. Aside of specific comments below, re-formatting of units, table layouts, etc., into one consistent format and re-structuring paragraphs may help to achieve this. As a general comment, the results section would benefit if the authors would focus on summarizing their main findings first, and discuss the limitations of the study in a second stage with a focus on their implications of the obtained results, rather than first discussing experimental conditions/limitations as results followed by reporting the actual findings.

In summary, I have enjoyed seeing these results and am looking forward to see the revised manuscript published.

The entire text was revised to improve clarity of the manuscript, shorten the text, and improve language where necessary. Some information was moved to the supplementary information in order to better emphasize the core findings in the manuscript text. The tables and figures have been reformatted where necessary for better consistency in formats. We also added a paragraph in the Results & discussion section which summarizes the main findings as requested by the reviewer.

SPECIFIC COMMENTS:

Overall:

The main findings are dilute throughout the manuscript and difficult to grasp. Parts in the conclusion section remain vague too. I suggest to summarize the main goals and questions of the study as specific as possible at the end of the introduction and to state the core findings as specific as possible in the conclusions section.

The goals of the manuscript are now stated more clearly at the end of Introduction. We included a chapter in the beginning of the Results and discussion to give an outline of the contents and major findings in the result:

"This study comprehensively characterises the chemical properties of RWC exhaust at different atmospheric aging times by combining extensive information gathered from gas-phase and particulate phase chemical analyses. In this section, we first discuss the dynamic combustion conditions and the characteristics of primary emissions from logwood stoves utilized with different fuels, which define the starting point for the aging experiments. Next, the aging conditions in the PEAR OFR are evaluated in order to validate the atmospheric relevance of the results. Finally, we assess the changes in the gaseous and particulate OA during the aging process under a variety of different oxidant concentrations. The observations of changes both in bulk- and molecular level aerosol chemical composition demonstrate that the major transformation pathway of OA changes from initial gas phase functionalisation followed by condensation to the transformation of the particulate OA by heterogeneous oxidation reactions and fragmentation. The study shows a linear dependency between OH exposure and organic aerosol oxidation state. Furthermore, OH-exposure-dependencies of specific OA constituents, such as nitrophenols, carboxylic acids and PACs, are established."

We also thoroughly revised the Conclusion section, where needed.

While the manuscript title is focused primarily on the photochemical aging of the emissions, a substantial part of the manuscript discusses primary emissions (Fig 2+3), operating/experimental conditions (Fig 4+5) and only the second part of figures (Fig 6-11) and results actually addresses the aging and chemistry question. In my view, some of the initial figures (e.g. 4+5) could be moved to the SI along with their text in favor of clarity of the manuscript; the implications of the determined losses in Fig 4+5 should then be referred to discussing the actual results, i.e. for example, the authors might adress how do particle/vapor losses influence the observed decay of compounds as a function of OH exposure in their experiments. Alternatively, Figure S1, S3 and S4 could fit well with the main text, as they summarize the primary emissions composition, which is relevant for any following discussion of emissions aging. Further remarks to help clarity and focus are listed later on.

We consider presentation of the primary emission contents important for throughout understanding of the aging process and products, but the focus of this manuscript is indeed in the secondary products formed in the aging exhaust. Thus, as proposed by the reviewer, revised Figure S3 was implemented in the main text, replacing previous, more general Figure 3. Furthermore, information on the LVOC fate, including previous Figures 4 and 5, was transferred to Supplementary section S2.2.

Abstract, Introduction & Methods:

- L20/ Abstract: suggest to specify here which oxidation flow reactor is used in this study; suggest to use "PEAR OFR" throughout

Revised as suggested by the referee. The reactor is now referred to as "the PEAR OFR" throughout the manuscript.

- L21 vs L 28 and other occasions/ Abstract: The authors mix between "gaseous organic compounds" and "volatile organic compounds"; suggest they try to harmonize the language

We harmonized the language by using "organic gaseous compounds (OGC)" throughout the manuscript when the volatility of the compound/group was not mentioned.

- L27/ Abstract: specify based on which analysis the acetic fragmentation is investigated

The following sentence was added into the abstract:

"Aging led to an increase in acidic fragmentation products in both phases, as measured by the IDTD-GC-ToFMS for the particulate and PTR-ToF-MS for the gaseous phase."

- L30 / Abstract and other occasions: the authors use the more generic term "polycyclic aromatic compounds (PACs)" rather than polycyclic aromatic hydrocarbons (PAHs) which has been used in previous related work and is also mentioned in e.g., L75. I suggest to specify and/or define for non-specialists, why the authors refer to PACs in some cases but PAHs in others. This should also take into account the limitations of their instrumentation to effectively distinguish between PACs and PAHs. In my understanding, frequently only fragments of PACs can be detected with PTR-ToF-MS or AMS, however, they are assumed to be and referred to as PAHs in the manuscript.

We chose to use the term "PAC" due to it covering also substituted polycyclic aromatic compounds. It is also suitable in cases where the parent compound is not known. The use of the terms (PAC/PAH) in the manuscript was revised to be more uniform (e.g. "*X-substituted PAC*" instead of "*X-substituted PAH*").

Analysis of all PACs, including the substituted PAHs, was done in similar manner. Fortunately, fragmentation of the PACs is minor in both PTR-ToF-MS (Gueneron et al., 2015) and AMS (Herring et al., 2015). With the AMS, the PAC with m/z < 300 are seen as the original molecular ion, while for larger PAC only the possible fragments are observed in the spectra (< 5 % of AMS signal; Herring et al. 2015). PACs are known to give intense signatures in AMS for both single and double charged molecular ions (Herring et al., 2015; Dzepina et al., 2007) due to delocalization of the charge, which is an asset when considering the extent of possible fragmentation. For the HR-PAH analysis, the quantification by the P-MIP-method (Herring et al., 2015) is done by considering also the main fragmentation and isotopic patters of the PACs, which enables precise molecular identification likewise for substituted and for hydrocarbon PACs.

- L36 / Abstract: suggest to specify which scale is "fresh", "shortly aged", and "longterm aged" in the context of this study

During revision, this sentence was removed from the abstract, which now states, more broadly, that "The observed continuous transformation of OA composition throughout a broad range of OH exposures indicates that the entire atmospheric lifetime of the emission needs to be explored --"

- L54: Is there a difference between "fresh" and "unaged"? Otherwise, I suggest the authors rephrase to read "fresh, i.e. not atmospherically aged"

In this situation there is no difference. Revised.

- L60/61: The authors may include in this section of SOA-precursor discussion that removing aromatic hydrocarbons from wood burning emissions by use of e.g. catalytic converters can drastically reduce SOA formation, as recently presented by Pieber et al., 2018; also changing applicance operation and modifying combustion phases to conditions that emit less aromatic hydrocarbons might have this effect; Figure S3+S4 are valuable indicators in this context.

This is a good notion, and now also included in the Introduction:

"-- removal of these [aromatic] compounds either via improved combustion conditions or for example catalytic cleaning have been shown to be efficient in lowering the SOA potential of RWC emissions (Czech et al., 2017; Pieber et al., 2018). "

It is now also mentioned in the results section 3.2.1 to highlight the importance of aromatic compounds to SOA formation.

- L87: suggest to provide some references for previous RWC OFR studies in addition to the men-tioned smog chamber experiments; e.g. Bruns et al. 2015, Czeck et al. 2017, Pieber et al. 2018, etc.

References to previous OFR studies are now also included.

- L132: "In addition". . . "additional"; language is redundant. Suggest to remove one of the two.

We have removed the extra "additional" as suggested.

- L133-134: Ozone and butanol-d9 metrics in volumetric flows does not provide any information on concentration levels; could the authors in addition or instead specify the mixing ratios?

Ozone mixing ratios are available in Table 1 and now also included in the Methods-section, together with the butanol-d9 mixing ratios.

- L134: "formed" should probably read "forms"

Corrected.

- L135: "depended" should probably read "depends"

Corrected.

- L135: "H2O" should probably read "H2O vapor"

Corrected.

- L143: "OH concentration" should read "24-hour average global OH concentration"

Corrected.

- L146: was butanol-d9 mixing ratio included in this equation an what is ist relative contribution to the total OHR external?

Butanol-d9 was not included in the initial OHRext calculations. We thank the reviewer for pointing this out, as naturally the additional OH tracer consumes radicals as well. The OHR_{ext} by butanol-d9 varied from 7 –17 s^{-1}, corresponding to 1 – 7 % of total OHR_{ext}. Its importance was highest on the experiments with otherwise lower OHR_{ext}, and minor (1 %) on the experiments with e.g. lower DR (and higher OHRext).

OHR_{ext} by butanol-d9 is now included in the discussion about OHR_{ext} and in the consideration of the reaction pathways in the PEAR OFR, including e.g. Table S4 and Figs. S6, S10 and S11.

- L148: suggest the authors present the main results of OHR external analysis in one brief sentence in this paragraph, and mention its implications for the results and conclusions later on.

We now present the main OHRext results already in the Methods Section 2.2:

"Due to the differences in the emission concentrations during logwood combustion also the OHRext , and consequently OHexp, vary also within a batch (Fig. S9). Average OHR_{ext} was in the range 130 – 1300 s-1 with the highest contributions from CO, NO, and unsaturated hydrocarbons (Fig. S5)."

- L150ff: suggest the author present the main results of particle and LVOC loss estimates in 1-2 brief sentences in the main text here and move the remaining text on this topic from the results section to the SI, discussing it in the main text only as a limitation of the study including its implications for conclusions (as reasoned above). I suggest also to define what LVOCs refers to in the context of this article.

Discussion of LVOC fate from chapter 3.3.1. was divided into main text Section 2.2. and SI Section S2.2. as suggested. We rephrased the whole paragraph, which now also better defines the meaning of "LVOC" in this context, i.e.: "The fate of the gaseous organic compounds capable of irreversible condensation under the present experimental conditions, i.e., low-volatility organic compounds (LVOC), was estimated based on Palm et al. (2016)".

- Line 160/161: I suggest to keep all information in one paragraph, rather than starting a new para-graph here.

Corrected as suggested.

- L167: suggest to define semi-VOCs in this context.

Section was revised to note that majority of the compounds can classified as semi- or intermediately volatile (saturation mass concentrations between 0.3 - 3×10^6), to highlight that these compounds may exist in both phases under the experimental conditions.

- L168: "isotope labelled" should probably read "isotopically labelled"

Corrected.

- L173: suggest to replace "after the PEAR" with "after the PEAR, i.e. at its outlet"

Revised to " -- were monitored at the outlet of the PEAR OFR"

- L187: the author refer to this instrument as "AMS" throughout the manuscript; I suggest to chan-ge this to SP-HR-ToF-AMS on all occasions, starting from the abstract, as is done for all other instrumentation (e.g. PTR-ToF-MS).

AMS is now referred to as SP-HR-TOF-AMS throughout the manuscript.

- L189: Why did the authors choose to use the "Improved-Ambient method" for this laboratory dataset?

The commonly used "Aiken-Ambient" method is systematically biased low (Aiken et al., 2008), with larger biases observed for alcohols and simple diacids. The Aiken-Ambient method underestimates the CO^+ and especially H_2O^+ produced many oxidized species. The Improved-Ambient method uses specific ion fragments as markers to correct for molecular functionality-dependent systematic biases and reproduces known O:C and (H : C) ratios of individual oxidized standards within 28 % (13 %) of the known molecular values (Canagaratna et al., 2015).

- L200: Suggest to compare also with Bruns et al., 2015 who have used this method beforehand for an intercomparison of spectra from OFR and smog chambers including RWC.

Bruns et al. (2015) applied the PMF as a tool for separation of POA/SOA components and created a two-factor solution by first finding the mass spectra for POA, and then assuming the rest as SOA (or aged-POA). In other words, spectra for SOA is not given nor were different oxidation pathways segregated. One important difference between PMF factors by Bruns et al. (2015) and those present here, is that in Bruns et al. the exhaust from the batch was first mixed in a chamber before aging in a PAM OFR, while in this manuscript the measurement of the exhaust was dynamic, and the factors are also tied to the combustion periods of batchwise combustion with the POA factors being separated by the combustion phases.

References to previous RWC studies utilizing similar factorization methods are now included in Section 2.5:

"Similar method have been used previously for example for the assessment of RWC generated POA and SOA in a chamber (Bruns et al., 2015a; Tiitta et al., 2016) and in an OFR (Bruns et al., 2015a) or for time-resolved analysis of RWC OA emission constituents (Elsasser et al., 2013; Czech et al., 2016). "

- L205: Suggest to replace "residential wood combustion" with RWC

Replaced as suggested.

- L209 (from L186 onwards): as noted in the next comments; please add important information on AMS data analysis in the main text.

Information of the AMS operating conditions was moved to the Material and methods Section S2.5.

Some text is repetitive or split into different locations (partially found in main text, partially in duplicate SI), while other text is grouped together into subchapters which are not entirely logical. I suggest to make the overall language more concise and shorten the text, while keeping all relevant information in the main text. E.g. some suggestions:

- L170 (main text): I suggest to relabel this as "Online aerosol particle and gas-phase measurements" to avoid ambiguity." It may be beneficial to split the subsection 2.4 into three sections for each instrument, and then make further separat paragraphs for any AMS in-formation aggregated as a) experimental/calibration/raw data correction, b) PMF analysis, c) HR fitting or PAH fitting.

We split the section 2.4 into two sections, namely, 2.4 for the gas phase measurements, 2.5. for the particulate-phase. AMS section now contains three paragraphs which are related to (1) data correction, (2) PMF-analysis, and (3) HR-PAH analysis.

- L186 onwards (main text): relevant AMS operating conditions (e.g. size-cut off) and data corrections (RIE=1.4 for OA, CO2+-interference correction, CO2 gasphase correction) should be mentioned in the main text; I suggest to move information from SI (Section S5) entirely to the main text, but shorten the paragraph by avoiding redundencies (e.g. "The AMS data was analysed using the standard analysis tools SQUIRREL v1.62A and PIKA v1.22D adapted in Igor Pro 8 (Wavemetrics)." is currently stated double.

Information of the AMS operating conditions was moved to the main text (Section 2.5) and the repetitive parts removed or rephrased; see specific comments for rephrased sections below.

- With regards to the RIE=1.4, please mention that this is valid for OA.

For biomass burning emissions, RIE of 1.4 agrees with the OA mass concentrations with stated ±38 % uncertainty of AMS (Bahreini et el., 2009; Xu et al. 2018). This is now stated in Section 2.5 discussing AMS analysis.

- With regards to the CO2+-interference correction, please mention the magnitude of interference and potential impacts on the determined O/C ratios.

A CO_2-AMS interference calibration value of 0.3 % (a=0.003) of the NO_3 concentration was determined by NO3NH4 calibration and corrected via the fragmentation table according to Pieber et al. (2016). Without correction, maximum effect on O:C value was 5 %, with typical values lying under 1 %. This is now stated in the Section 2.5 on AMS analyses.

- What was the level of inorganic nitrate to OA in the primary and secondary emissions?

The concentrations of inorganic NO_3 in the emissions are available in Table S7. The ratio of NO_3-to-OA varied between 0.02 (masonry heater, age 1.5 eqv.d) and 1.1 (chimney stove, age 0.6 eqv.d), but cannot be tied to atmospheric age. As stated in the previous answer, the effect of nitrate to the AMS analysis was small.

- With regards to CO2 gas phase-correction, please mention whether this was done by standard measurements of particle-filtered air during the experiment or external calibration with gaseous CO2.

The time-dependent gas-phase CO_2^+ subtraction was applied. It was conducted using the online HEPA filter measurement technique of gas-phase CO_2 for corrections. This information was added to the Material and methods Section 2.5 on AMS analysis.

- L190 onwards (main text): I suggest to make a new paragraph with all information relevant to PMF, see comments above.

The information considering PMF was separated into its own paragraph, as suggested by the reviewer.

Results:

- L210: Suggest to relabel as "results and discussion", given the separate section entitled "conclusions" in L540

Corrected.

- Section 3.1.: Is there any information on the temperatures during these different combustion phases available?

Unfortunately, no measured temperature information is available from the current study. The time-dependent temperature patterns during batchwise logwood combustion and their effects on emission characteristics have been established earlier by e.g. Czech et al., (2016) and Kortelainen et al., (2018). Section 3.1 was modified to not give an impression that we have exact measured temperature data available from these experiments.

- L228: "constantly" should probably read "continuously"; "from the diluted flue gas" should pro-bably read "in the diluted flue gas".

Corrected.

- L232: "primary aerosol" is certainly technically correct if referring to aerosol as particles plus their surrounding gas, however, it may quickly become confusing as often "aerosol" is used when refer-ring to the particle phase only. I suggest to replace "primary aerosol" with "primary emissions" here.

This sentence was revised to "-- OGC in the primary emissions --" to highlight that here we discuss the gaseous phase of the primary emissions.

- L233: suggest to specify the value of protonation efficiency (proton affinity) here

Mention of the exact proton affinity of water (691 kJ mol^{-1}) that sets apart the detectable compounds is now included.

o L230: suggest to state the limitations of both, FTIR and PTR-ToF-MS, here briefly, e.g. for PTR-ToF-MS, rather than point out alkanes specifically, it should be noted that any molecules with proton affinity lower than that of water (in H3O+ mode) can not be protonated and hence detected; further, I suggest to mention based on which criteria 127 molecular formulas were identified and how many ions remained unidentified. For the FTIR, it would be informative to give a brief reasoning why only 27 compounds can be detected and quantified, rather than only refer to the table in SI.

The sentence about PTR limitations is now revised, including e.g. the limiting protonation affinity, as suggested. The identification of compounds by PTR-MS was done based on the high-resolution m/z and previously reported compounds found from RWC as in previous work (Hartikainen et al. 2018) as stated on Section 2.4. Molecular formula could be allocated to majority of the compounds, although precise identification of higher m/z compounds is innately not possible.

The organic compounds measured with the FTIR were limited to those calibrated to the particular instrument used in this study. The sentence describing the measured components in the manuscript Section 3.2.1 now states that "-- FTIR was calibrated for 27 typical combustion-derived compounds --"

- L233: fragmentation does not necessarily limit the quantification but rather the identification; suggest to rephrase

True. The sentence is rephrased.

- L236: suggest to introduce the later used abbreviation "ArHC" here at its first occasion

Introduction of the abbreviation is now included already in Section 3.2.1.

- L243: suggest to replace "significant" by "statistically significant" here

Done.

- L259: ArHC are also discussed earlier, but the abbreviation is only introduced in L259; suggest to revise and use and define ArHC earlier on

ArHC is now defined already in the Section 3.2.1 when discussing primary OGC emissions.

- L265: Suggest to add that previous studies (e.g. Pieber et al. 2018), demonstrated that removing ArHC from the emissions mix substantially reduces their SOA formation.

A notion that " removal of ArHC from the flue gas either by improving combustion conditions or using e.g. catalytic cleaning has been noted to decrease also the resulting SOA formation (Bruns et al., 2016; Hartikainen et al., 2018; Pieber et al., 2018). " were added to Section 3.2.1, as suggested.

- Figure 7 and 8: where do O/C and H/C ratios of other wood burning OFR studies fall in compari-son to the obtained results (e.g. add data from Bruns et al., 2015, Czech et al. 2017, Pieber et al., 2018, and similar data from other research groups as available).

The OSc of highly aged particulate OA observed here is lower than previously measured for RWC exhaust with a PAM OFR (Bruns et al., 2015, Pieber et al., 2018), where the exhaust from batchwise combustion was mixed prior to aging in the PAM. While this approach is reasonable as the exhaust exists as a mixture also in the atmosphere, the resulting O:C and H:C ratios (see the van Krevelen-diagram below (Fig. 6 in the revised manuscript)) indicate worse agreement with the ambient range when compared to compositions obtained by the PEAR OFR (presented in this work) or previously measured in a chamber (Tiitta et al., 2016). This can also be due to differences in the combustion technologies and protocols or differences in the aging conditions.

Comparison of the O:C and H:C ratios of the particulate OA to previous studies in the Section 3.5.1 is now expanded. The results of aging of RWC exhaust by PAM OFR (by Bruns et al., 2015 and Pieber et al., 2018) are included also in the van Krevelen diagram (previously Fig. 8, now Fig. 6). Values from Czech et al. (2017) were not included in the van Krevelen diagram due to different combustion source (pellet boiler with notably higher initial oxidation states) but are included in the discussion on OS_C on Section 3.5.1.

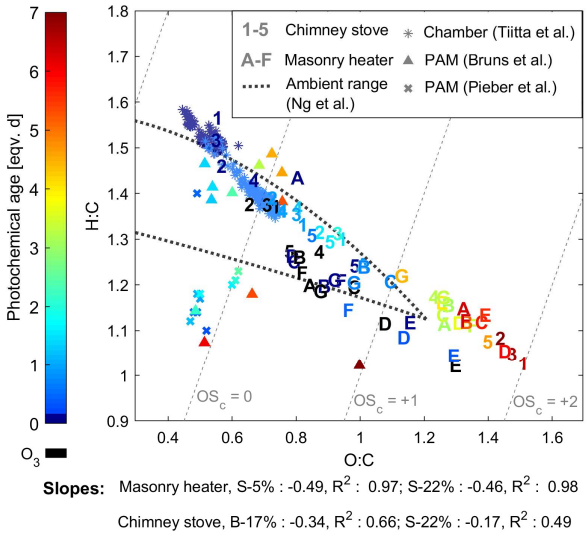

Regarding the gaseous phase (Previous Fig. 7, now Fig. 5), OFR studies reporting gaseous compounds from RWC extensively are scarce and direct comparison of O:C and H:C ratios is not possible due to e.g. differences in the analyzed and reported compounds. Previously, Bruns et al. (2017) have reported emission factors for primary and secondary exhaust for 65 compounds measured with a PTR-MS. Although these compounds differ slightly from those considered here, the main compounds (aromatics and carbonyls with highest concentrations) are included. The changes during aging reported by Bruns et al. (2017) follow the phenomena observed here: both O:C and H:C ratios increase by photochemical exposure. The ΔH:C/ΔO:C during the five chamber experiments in Bruns et al. (2017) are in the range of 0.34 - 0.81 at final exposure of 1.9-2.3 eqv.d, which is similar to the changes observed here. This is now noted also in Section 3.4.

- L371: Replace "consequent" with "subsequent"

Corrected.

Conclusions

- L556: "Notably, small, acidic" should probably read "Notably, small acidic" (i.e. without comma)

Corrected.

- L565: given that the presented manuscript discusses OFR-experiments, I suggest to cite and discuss also other OFR studies with RWC rather than only smog chamber experiments; e.g. Czech et al. 2017, Bruns et al. 2015, Pieber et al. 2018: how do those PAM OFR studies compare in OH exposure with the here presented PEAR OFR study?

The photochemical exposures were in the ranges 0.5-2.5 eqv.d in Pieber et al. (2018) and ~18 eqv.h in Czech et al. (2017) who discuss pellet burning. To our knowledge, highest OH exposures for RWC exhaust in a PAM have been reported by Bruns et al. (2015), where the exposure was 2.5-10 eqv.d for the flaming phase of RWC.

The conclusions section was overall revised, including rephrasing of this paragraph and addition of references to OFR studies, which are now also otherwise better noted in this work.

L564-566: The authors conclude: "Based on this work, different transformation pathways for RWC exhaust under photochemical conditions can be roughly outlined: the initial pathways consisting of functionalisation and condensation from gaseous precursors are followed by more particulate-phase-driven chemistry consisting of heterogeneous oxidation and fragmentation." The authors need to discuss their limitations of differentiating between gas-phase oxidation, heterogeneous chemistry and particle phase- driven chemistry owing to their experimental set-up in the discussion of the results and the presentation of their conclusions.

Limitations in differentiating between gas-phase oxidation, heterogeneous chemistry and particle phase -driven chemistry certainly exist. In addition, it should be noted that the different oxidation processes are likely overlapping. The sentence in question was aimed to simply give a rough outline of the major oxidation mechanisms, and is based on the following facts observed in this study: (1) for RWC-exhaust, short OH-exposures are sufficient to functionalize gaseous precursors and lead to their condensation into particulate phase, which consequently dominates the overall OA transformation until the SOA precursors have been depleted; (2) continuing aging in the presence of OH-radicals leads to further oxidation of particulate organic aerosol, which is likely explained by heterogenous reactions between gas-phase oxidants and particles. However, related to the second fact it is also possible that particulate phase oxidation occurs via evaporation and homogeneous gas-phase oxidation followed by recondensation, as discussed by for example Tiitta et al. (2016). Third, it should not be omitted that in an OFR utilized with high OH-radical concentrations, the gaseous phase precursors may receive higher oxidation state before condensation, e.g. due to several fast functionalization reactions in the gas phase, which would be a topic for further studies. Nevertheless, the comparison of similar OH-exposure in a smog chamber (low OH-radical concentrations) and the PEAR OFR (high OH-radical concentrations) give fairly similar OA oxidation states, as stated e.g. in Section 3.5.1. and shown in Figure 6 (van Krevelen -diagram). This indicates that the utilized high OH-concentrations do not lead to any severe artefacts in terms of OA composition.

We have revised the text in the Conclusions section to better reflect on the limitations and the observations on which the conclusions are based upon.

- L569 onwards: this information is quite generic and could be omitted and replaced with more specific conclusions in my point of view; otherwise it does not add additional value to the manuscript.

This last, concluding paragraph considers the potential uses of these results, especially the importance of the consideration of different atmospheric aging stages for OA. The aim of the section in question is to emphasize the need for similar consideration of also other OA sources as a point toward future studies, pointing also towards the potential importance of aging towards both environmental and health related effects.

We have revised this final section of the Conclusions section, which now reads:

"--this study highlights the importance of also higher exposure levels towards chemical transformation of OA. Due to the potentially long atmospheric lifetimes of OA, long-term aging is also important to consider in large-scale atmospheric models, which typically estimate SOA formation and characteristics based on short-term aging experiments. The consideration of only the first stage of gas-phase functionalization and condensation may lead to underestimated oxygenation of the long-transported OA, while specific compound groups, such as nitrophenols or substituted-PACs, can be overestimated. In general, the potential health and climate effects of aerosols are to a large extent determined by their composition, which depends on their sources and the levels of atmospheric aging. Thus, the characterisation of aerosol emissions from different sources and their atmospheric transformation at different exposure levels would be crucial for assessment of the overall environmental effects of ambient air pollution."

Technical Comments

- Formatting of units (e.g. L/min vs L min-1), figures (e.g. legends are sometimes to be found left, right or centered) and tables (e.g. horizontal lines in tables, as well as table dimensions), in particular in the SI is inconsistent. While this is of course not critical with regards to the scientific quality of the work, it would help the reader to follow the presented research work more easily and hence enjoy the results more.

The notations for units were corrected. Tables were made more consistent with e.g. no horizontal lines, and the figures were revised for better coherency, with similar formatting of figures of similar type (e.g. scatterplots Figs. 9-10 or timeseries in Figs. S6 and S10-S11.

Supporting Information

- All information provided in the SI should also be noted in the main text; all information provided in the SI should be described with the references such that the document can be read independently, etc.

All portions of SI are noted in the main text and clarification and references included in the text where needed.

- E.g., Table S1: please add reference for the OH constant used.

Reference included.

- E.g. Table S2.1: please add reference for the "OHR external" definition. Is CH4 negligible or why was it not included in the analysis?

Reference to the OHR_{ext} is now included on Table S2.1. Methane (CH_4) is included in the analysis (6^{th} compound from the bottom of the Figure S2), although its share in the total OHR_{ext} is minor (< 0.025 %) due to its low OH reactivity.

REFERENCES

Bruns et al. 2015, DOI: 10.5194/amt-8-2315-2015 Czech et al. 2017, DOI:

10.1016/j.atmosenv.2017.03.040 Pieber et al. 2018, DOI: 10.1021/acs.est.8b04124

REFERENCES

Aiken, A. C., DeCarlo, P. F., Kroll, J. H., Worsnop, D. R., Huff-man, J. A., Docherty, K. S., Ulbrich, I. M., Mohr, C., Kimmel, J. R., Sueper, D., Sun, Y., Zhang, Q., Trimborn, A.,Northway, M., Ziemann, P. J., Canagaratna, M. R., Onasch,T. B., Alfarra, M. R., Prevot, A. S. H., Dommen, J., Duplissy,J., Metzger, A., Baltensperger, U., and Jimenez, J. L. O/C and OM/OC Ratios of Primary, Secondary, and Ambi-ent Organic Aerosols with High-Resolution Time-of-Flight Aerosol Mass Spectrometry. Environ. Sci. Technol., 42, 4478–4485, doi:10.1021/es703009q, 2008.

Bahreini, R., Ervens, B., Middlebrook, A. M., Warneke, C., de Gouw, J. A., DeCarlo, P. F., Jimenez, J. L., Brock, C. A., Neuman, J. A., Ryerson, T. B., Stark, H., Atlas, E., Brioude, J., Fried, A., Holloway, J. S., Peischl, J., Richter, D., Walega, J., Weibring, P., Wollny, A. G., and Fehsenfeld, F. C. Organic Aerosol Formation in Urban and Industrial Plumes near Houston and Dallas, Texas. J. Geophys. Res. Atmos, 114, doi:10.1029/2008JD011493, 2009.Canagaratna et al., 2015.

Bruns, E. A., El Haddad, I., Keller, A., Klein, F., Kumar, N. K., Pieber, S. M., Corbin, J. C., Slowik, J. G., Brune, W. H. and Baltensperger, U. and Prévôt, A. S. H.: Inter-comparison of laboratory smog chamber and flow reactor systems on organic aerosol yield and composition, Atmos. Meas. Tech, 8, 2315-2332, doi:10.5194/amt-8-2315-2015, 2015.

Bruns, E. A., Slowik, J. G., El Haddad, I., Kilic, D., Klein, F., Dommen, J., Temime-Roussel, B., Marchand, N., Baltensperger, U. and Prévôt, A S H: Characterization of gas-phase organics using proton transfer reaction time-of-flight mass spectrometry: fresh and aged residential wood combustion emissions, Atmos. Chem. Phys., 17, 705-720, doi:10.5194/acp-17-705-2017, 2017.

Czech, H., Sippula, O., Kortelainen, M., Tissari, J., Radischat, C., Passig, J., Streibel, T., Jokiniemi, J. and Zimmermann, R.: On-line analysis of organic emissions from residential wood combustion with single-photon ionisation time-of-flight mass spectrometry (SPI-TOFMS), Fuel, 177, 334-342, doi:10.1016/j.fuel.2016.03.036, 2016.

Dzepina, K., Arey, J., Marr, L. C., Worsnop, D. R., Salcedo, D., Zhang, Q., Onasch, T. B., Molina, L. T., Molina, M. J. and Jimenez, J. L.: Detection of particle-phase polycyclic aromatic hydrocarbons in Mexico City using an aerosol mass spectrometer, International Journal of Mass Spectrometry, 263, 152-170, doi:doi:10.1016/j.ijms.2007.01.010, 2007.

Hartikainen, A., Yli-Pirilä, P., Tiitta, P., Leskinen, A., Kortelainen, M., Orasche, J., Schnelle-Kreis, J., Lehtinen, K. E., Zimmermann, R., Jokiniemi, J. and Sippula O.: Volatile organic compounds from logwood combustion: emissions and transformation under dark and photochemical aging conditions in a smog chamber, Environ. Sci. Technol., 52, 4979-4988, doi:10.1021/acs.est.7b06269, 2018.

Kortelainen, M., Jokiniemi, J., Tiitta, P., Tissari, J., Lamberg, H., Leskinen, J., Rodriguez, J. G., Koponen, H., Antikainen, S., Nuutinen, I., Zimmermann, R. and Sippula, O..: Time-resolved chemical composition of small-scale batch combustion emissions from various wood species, Fuel, 233, 224-236, doi:10.1016/j.fuel.2018.06.056, 2018.

Pieber, S. M., El Haddad, I., Slowik, J. G., Canagaratna, M. R., Jayne, J. T., Platt, S. M., Bozzetti, C., Daellenbach, K. R., Fröhlich, R., Vlachou, A., Klein F., Dommen, J., Miljevic, B., Jiménez J. L., Worsnop D. R., Baltensperger, U. and Prévôt A. S. H.: Inorganic salt interference on CO2 in aerodyne AMS and ACSM organic aerosol composition studies, Environ. Sci. Technol., 50, 10494-10503, doi:10.1021/acs.est.6b01035, 2016.

Pieber, S. M., Kambolis, A., Ferri, D., Bhattu, D., Bruns, E. A., Elsener, M., Kröcher, O., Prévôt, A. S. and Baltensperger, U.: Mitigation of Secondary Organic Aerosol Formation from Log Wood Burning Emissions by Catalytic Removal of Aromatic Hydrocarbons, Environ. Sci. Technol., 52, 13381-13390, doi:10.1021/acs.est.8b04124, 2018.

Xu, W., Lambe, A., Silva, P., Hu, W., Onasch, T., Williams, L., Croteau, P., Zhang, X., Renbaum-Wolff, L., Fortner, E., Jimenez, J. L., Jayne, J., Worsnop, D. and Canagaratna, M.: Laboratory evaluation of species-dependent relative ionization efficiencies in the Aerodyne Aerosol Mass Spectrometer, Aerosol Sci. Tech., 52, 626-641, doi:10.1080/02786826.2018.1439570, 2018.

Anonymous Referee #2

Overview

The manuscript by Hartikainen et al investigates how gas- and particle-phase emissions from residential wood combustion vary with respect to combustion conditions (including stove type) and fuel. Additionally, the emissions are aged in a photochemical reactor to investigate how composition evolves with atmospheric age. Numerous analytical techniques are used allowing the authors to broadly characterize both gases and aerosols. Overall, the authors find that emissions depend on combustion conditions and that photochemical aging alters composition, generally by creating more oxidized species. Emissions from residential wood combustion is an important and poorly understood contributor to air quality issues and the understanding of the influence of aging is poor. Thus, although this is a largely descriptive paper with few quantitative or testable conclusions, the experiments are of interest to the community. However, I have several major concerns that should be addressed prior to acceptance. My main critique is that the manuscript claims to investigate the aging that occurs over multiple days but there is no discussion about how the experimental conditions differ from the atmosphere nor is there discussion/consideration about how important reactions such as peroxy radical fate differ between the OFR and the real atmosphere.

Major Comments

1) The description and analysis of the OFR experiments is insufficient and requires substantial expansion. Interpreting the chemistry of OFRs is difficult and there needs to be careful consideration of the dilution effects, gas-phase peroxy radical fate, NO and NO2 mixing ratios, and potential for unwanted chemistry if the results are to be applied to the atmosphere. This is particularly true when making claims about multiple day aging timescales as is done here.

In terms of the description, details such as the mixing ratio of ozone and butanol should be included as should the residence time. In terms of analysis, the authors need to more carefully consider the operation of the OFR, how this impacts the results, and the subsequent implications for atmospheric relevance. I list some specific questions below, but there needs to be a more general consideration of this chemistry.

Description of the aging conditions and reactor use is naturally crucial for an OFR study, and consideration of the questions pointed out by the reviewer clearly improves the credibility of this assessment in this manuscript. In the following sections we provide point-to-point answers to the specific questions presented by dividing the comments by topic.

Mixing ratios of O_3 (2-11 ppm) are included in Table 1, and are now indicated more pronouncedly in the text of Material and methods Section 2.2 together with the initial mixing ratio of butanol-d9, which was 80-200 ppb. Residence time (139 s) is now also stated clearly in the Section 2.2.

For instance, in the atmosphere the emissions will experience dilution over the course of several days aging – how might dilution alter the implications of this work?

Dilution has important impacts to the gas-particle partitioning of organic aerosol. Under higher dilutions, semivolatile compounds measured in this work would have had higher concentrations in the gas phase and, in turn, lower concentrations in the particulate phase from where they were assessed with the IDTD-GCMS. During the lifetime of the emissions from the emission source until long-range transported smoke, a high range of different dilution ratios exist. For practical reasons (e.g. limited measurement time), we could perform the experiment only by using a certain range of dilution ratios. The usage of very high dilution ratios, which would be most representative to atmosphere, would be possible to in the OFR, but it would hamper the possibilities for comprehensive chemical and physical analyses of aerosols, due to sensitivity limits of the instruments. Thus, we used lower dilution in the PEAR than what normally occurs in atmosphere but have the advantage of better quality in the chemical analysis results. This is now mentioned also in the text (Section 3.3).

How representative is the peroxy radical chemistry (Peng et al., 2019) and how might this alter in particular the gas-phase measurements?

Due to the high OH and HO_2 concentrations in the PEAR OFR, the shortened lifetime of RO_2 decreases its isomerization compared to atmospheric conditions (Peng et al., 2019). Further, the HO2-to-OH ratio (roughly approximating in the range of ~10-50:1) is lower than in atmosphere (~100:1). Consequently, the importance of RO_2+OH reactions is enhanced. The RO_2 fate in the PEAR OFR was roughly estimated using the RO_2 fate estimator by Peng et al. (2019). The estimation of the RO_2 fates during the first minute, during which majority of the OGC have reacted, is given below for two different experiments: first with high OH exposure (Masonry heater Exp. 2), second with high OHR_{ext} (Chimney stove Exp. 5).

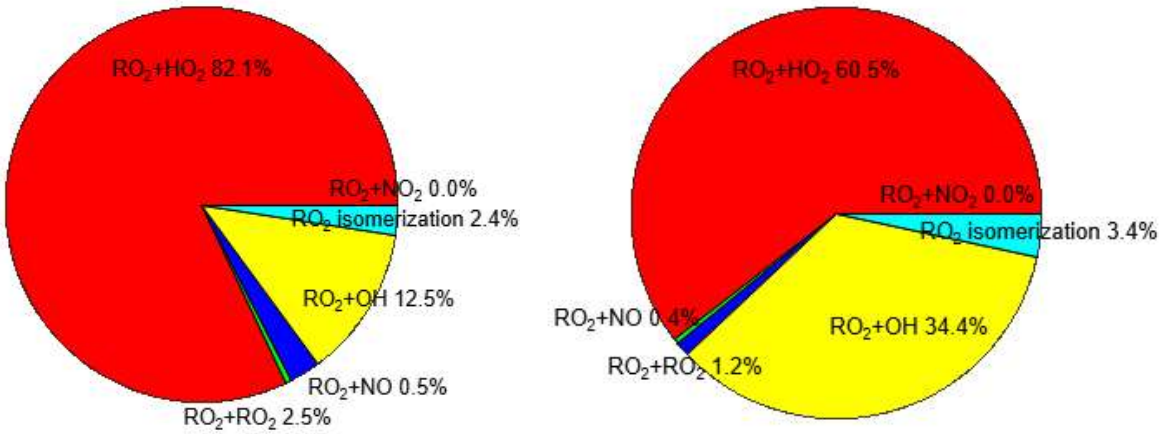

Discussion of the peroxy radical chemistry is now included in Section 3.3 discussing OFR chemistry and noted also in the discussion of VOC transformation, as fragmentation in the PEAR OFR may be enhanced due to the different RO_2 chemistry than in atmosphere or in chamber experiments.

Is NO_3 chemistry occurring in the reactor and if so, does it vary as a function of the OH exposure or across a given experiment?

We assume NO_3 to be negligible due to its slow formation rate and fast photolysis in the PEAR. This is supported by the low AMS NO-to-NO_2 ratio, based on which all particulate nitrate was inorganic.

The formation of compounds such as nitroaromatics will depend on NO2. Is it possible that nitrophenols decreased with increased aging because the NO/NO2 chemistry was altered in the reactor and thus the formation of nitrophenols was altered (rather than nitrophenols being oxidized by the increased OH as is implied in the manuscript)?

Although the ratio of NO-to-NO_2 prior to aging was in the range of ~10-40:1, NO is rapidly oxidized to NO_2 in the PEAR OFR and the amount of NO measured downstream the PEAR OFR is negligible (<0.02 ppb) in all experiments. Similar NO-to-NO_2 conversation takes place also in environmental chamber, where formation of nitrophenols has been observed previously (Hartikainen et al., 2018). Furthermore, exposure level was not observed to affect the observed NO_2 levels.

Although we cannot explicitly state the reason for nitrophenol decay in the scope of this manuscript, we find it likely that the after the rapid conversion of the precursor compounds (i.e., phenols) has taken place at the first stages of aging, the change in nitrophenol concentrations in the PEAR OFR is governed by nitrophenol-OH reactions and photolysis (Hems and Abbatt, 2018), which are both enhanced in the high-aging experiments due to the high photon fluxes and OH concentrations.

Overall, the OFR chemistry needs to be considered more thoroughly in order for meaningful conclusions to be drawn about how the emissions will be transformed in the atmosphere.

We hope that the above-mentioned improvements on the explanations of the chemistry in the PEAR OFR and the overall revision of the manuscript text now provide satisfactory information for validation of the used method and comparison against atmospheric conditions.

2) I find the manuscript difficult to read given the number of different variables explored and the number of analytical techniques used. While it is an advantage that multiple instruments measured the same thing, it is often not clear in the figures or the text which measurement or condition is being discussed. This makes it difficult for the reader to identify the main conclusions and findings. Clarification of the combustion/oxidation conditions and analytical instrumentation being discussed needs to be made more explicit throughout the text. For instance, in Fig. 6 are the values averaged over all the batches? I assume that Fig. S2 is FTIR measurements, but it would be useful to explicitly state.

In Figure 6 (now Fig. 4) the values are indeed averaged over all the batches per experiments and Fig. S2 is based on the FTIR measurements. Clarification of the conditions and analytical instrumentation employed for

each finding was added when necessary, for example in Sections 3.5.4 and 3.5.5 and in the supplementary figures (Figs. S2, S5-S8, S16-S17 and S19).

Minor Comments

Sect 3.5.2 Did the authors consider performing PMF with the rBC peaks included? It would be interesting to see if the rBC peaks supported the PMF factor interpretation.

We thank referee for the valuable idea of performing PMF analyses with the rBC peaks included. However, it falls outside of the main focus of this paper, which is the dependence of organic aerosol composition on OH exposure.

We performed a test run with PMF applying SP-AMS data using refractory carbon clusters. Two-factor solution showed that timeseries of the rBC-dominated factor correlated best with the timeseries of flaming-BBOA factor (see figure below). This observation supports the PMF interpretation since it is well-known that the refractory black carbon is formed mainly during the flaming phase (Kortelainen et al., 2018; Nielsen et al., 2017).

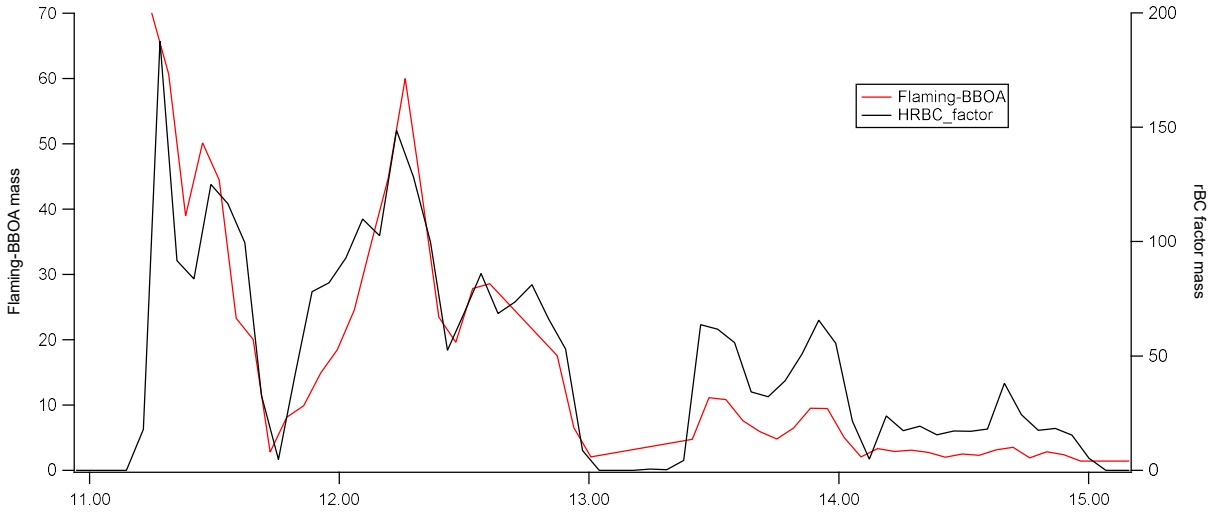

In future work we would also like to connect refractory black carbon with the high-resolution NR-OA to analyze rBC-associated coating of OA.

Line 494: The statement about diminished health effects is not well supported, particularly since it is followed with a statement that the heteroatom containing PACs may have negative health impacts. Without any measurements of for instance ROS generation, I think the more accurate statement is that the health effects would likely change (but no indication of better or worse).

True. This sentence in Section 3.5.3 was revised, and now reads:

"The change in the PACs also alters the potential health effects of the exhaust: although the total PAC concentration decayed, the simultaneous formation of oxy- and nitro-PAC derivatives known to be detrimental to health was observed."

Technical comments

Why only consider m/z 40-180 for the PTR?

According to our experience, the compounds reliably measurable from RWC exhaust with PTR fall within this range, which was stated mainly to specify the observable range to the reader. The sentences in Section 3.2.1 and 3.4. describing the use of PTR-MS are now rephrased ("-- for OGC in the primary emissions were identified in the m/z range of 40–180 --" and "aging may also lead to the growth of compounds outside the observable mass range", respectively).

I think "oxygenated" rather than "oxidized" would be a better choice for describing the compounds measured in the unoxidized exhaust in order to avoid confusion (for instance in Fig. S3).

This is true. We also used "oxygenated" instead of "oxidized" in the text and for example in the previous Fig. 3 and Table S1. The description is now unified and "oxygenated" used also in e.g. Fig. S2 and the previous Fig. S3 (now revised and replacing Fig. 3 in the main text).

S3 and S4 are difficult to interpret since the x-axis and groupings are changed. It would be easier to compare if they were kept in the same format.

Figure S3 was revised to share the format of Fig. S4 (now S3) and moved to the main text where it now replaces the previous Fig. 3.

Line 65 and elsewhere, please clarify what is meant by "semi-VOCs"

Rephrased to more general term, organic gaseous compound (OGC).

Line 267 these aren't units of emissions

We revised the terminology to "concentrations" in this section (3.2.2) considering the primary emissions. The concentrations in the secondary exhaust are normalized to 13 % flue gas excess oxygen, which is a common procedure to present emissions from logwood fired stoves. The fact that the emission concentration is normalized to a certain oxygen level means that the values corrected for the changing air-to-fuel ratios and are therefore directly proportional to emission factors as #/fuel energy content or #/consumed fuel mass. The emission factor calculation procedures are presented more thoroughly by e.g. Reda et al., (2015, supplement). We have now also stated clearly in e.g. figures which concentrations are normalized to 13% flue gas excess oxygen.

Line 287: Figure S14 referenced out of order. Other references may be out of order as well.

Due to the length of the supplementary information, it is structured by subject matter. In other words, all material related to each subject are all grouped under the respective title, rather than included in the order of first appearance. We also decided to keep figures with the same structure/topic together, which is the case with Fig. S14 (now Fig. S15), where thermal-optical EC and OC are compared to AMS rBC and OA, respectively.

In some cases, this also leads to references in the main text to be out of order. With this, we aim to help the reader in finding the information related to each subject.

Line 319: What is meant by “external OH reactivity”?

External OH reactivity refers to the OH reactivity of the gases in the sample that is input PEAR OFR (Li et al., 2015). It is defined in the Material and methods section 2.2.

Reference Peng, Z., Lee-Taylor, J., Orlando, J. J., Tyndall, G. S. and Jimenez, J. L.: Organic peroxy radical chemistry in oxidation flow reactors and environmental chambers and their atmospheric relevance, Atmospheric Chem. Phys., 19(2), 813–834, doi:https://doi.org/10.5194/acp-19-813-2019, 2019.

REFERENCES

Hartikainen, A., Yli-Pirilä, P., Tiitta, P., Leskinen, A., Kortelainen, M., Orasche, J., Schnelle-Kreis, J., Lehtinen, K. E., Zimmermann, R., Jokiniemi, J. and Sippula O.: Volatile organic compounds from logwood combustion: emissions and transformation under dark and photochemical aging conditions in a smog chamber, Environ. Sci. Technol., 52, 4979-4988, doi:10.1021/acs.est.7b06269, 2018.

Hems, R. F. and Abbatt, J. P.: Aqueous phase photo-oxidation of brown carbon nitrophenols: reaction kinetics, mechanism, and evolution of light absorption, ACS Earth Space Chem., 2, 225-234, doi:10.1021/acsearthspacechem.7b00123, 2018.

Kortelainen, M., Jokiniemi, J., Tiitta, P., Tissari, J., Lamberg, H., Leskinen, J., Grigonyte-Lopez Rodriguez, J., Koponen, H., Antikainen, S., Nuutinen, I., Zimmermann, R., and Sippula, O.: Time-resolved chemical composition of small-scale batch combustion emissions from various wood species. Fuel 233, 224-236, doi:10.1016/j.fuel.2018.06.056, 2018.

Li, R., Palm, B. B., Ortega, A. M., Hlywiak, J., Hu, W., Peng, Z., Day, D. A., Knote, C., Brune, W. H., De Gouw, J. A. and Jimenez, J. L.: Modeling the radical chemistry in an oxidation flow reactor: radical formation and recycling, sensitivities, and the OH exposure estimation equation, The Journal of Physical Chemistry A, 119, 4418-4432, doi:10.1021/jp509534k, 2015.

Nielsen, I. E., Eriksson, A.C., Lindgren R., Martinsson, J., Nyström, R., Nordin, E. Z., Sadiktsis, J., Boman, C., Nojgaard, J. K., and Pagels, J.: Time-resolved analysis of particle emissions from residential biomass combustion – Emissions of refractory black carbon, PAHs and organic tracers. Atm. Environ. 165, 179-190, doi:10.1016/j.atmosenv.2017.06.033, 2017.

Peng, Z., Lee-Taylor, J., Orlando, J. J., Tyndall, G. S. and Jimenez, J. L.: Organic peroxy radical chemistry in oxidation flow reactors and environmental chambers and their atmospheric relevance, Atmospheric Chem. Phys., 19(2), 813–834, doi:10.5194/acp-19-813-2019, 2019.

Reda, A. A., Czech, H., Schnelle-Kreis, J., Sippula, O., Orasche, J., Weggler, B., Abbaszade, G., Arteaga-Salas, J., Kortelainen, M., Tissari, J., Jokiniemi, J., Streibel, T. and Zimmermann, R.: Analysis of Gas-Phase Carbonyl Compounds in Emissions from Modern Wood Combustion Appliances: Influence of Wood Type and Combustion Appliance, Energy Fuels, 29, 3897-3907, doi:10.1021/ef502877c, 2015.

Changes made to the manuscript "Photochemical transformation of residential wood combustion emissions: dependence of organic aerosol composition on OH exposure" during revision

Abstract. Residential wood combustion (RWC) emits large amounts of gaseous and particulate organic aerosol (OA). In the atmosphere, the emission is transformed via oxidative reactions, which are under daylight conditions driven mainly by hydroxyl radicals (OH). This continuing oxidative aging produces secondary OA and may change the health- and climate-related properties of the emission. However, it is not well known how the composition of RWC-originated OA changes as the function of OH-exposure. In this work, emissions from two modern residential logwood combustion appliances were photochemically aged in an oxidation flow reactor (PEAR OFR) with various OH exposure levels, reaching up to 6×10^{11} s cm^{-3} (equivalent to one week in the atmosphere). Gaseous organic compounds were analysed by proton transfer reaction time-of-flight mass spectrometry (PTR-ToF-MS), while particulate OA was analysed online by an aerosol mass spectrometer (SP-HR-ToF-AMS) and offline by thermal-optical analysis and thermal desorption-gas chromatography mass spectrometry. (IDTD-GC-ToFMS). Photochemical reactions increased the mass of particulate organic carbon by a factor of 1.3–3.9. The increase in mass took place during the first atmospheric equivalent day of aging, after which the enhancement was independent of the extent of photochemical exposure. However, aging increased the oxidation state of the particulate OA linearly throughout the assessed range, with ΔH:C/ΔO:C slopes between -0.17 and -0.49 in van Krevelen space. Aging led to an increase in acidic fragmentation products in both phases., as measured by the IDTD-GC-ToFMS for the particulate and PTR-ToF-MS for the gaseous phase. For the volatilegaseous organic compounds measured by PTR-ToF-MS, the formation of small carbonylic compounds combined with the rapid degradation of primary volatile organic compounds such as aromatic compounds led to a continuous increase in both the O:C and H:C ratios. Overall, the share of polycyclic aromatic compounds (PACs) in particles degraded rapidly during aging, although some oxygen-substituted PACs, most notably naphthaldehydic acid, increased, in particular during relatively short exposures. Similarly, the concentrations of particulate nitrophenols rose extensively during the first atmospheric equivalent day. During continuous photochemical aging, the dominant reactiontransformation mechanisms shifted from the initial gas phase functionalisation/condensation to the transformation of the particulate OA by further oxidation reactions and fragmentation. The observed continuous transformation of OA composition throughout a broad range of OH exposures indicates that the entire atmospheric lifetime of the emission, from fresh to shortly aged to long-term aged emission (representative of long-range transported pollutants), needs to be explored to fully assess the potential climate and health effects of OARWC emissions.

1 Introduction

Biomass combustion is a major source of atmospheric particulate matter (PM) and is considered the main anthropogenic source of organic matter and the third largest contributor of black carbon (BC) emissions globally (Klimont et al., 2017). The use of wood fuels in small-scale residential settings is a main source for ambient organic aerosol (OA) in many parts of the world. For example, residential wood combustion (RWC) has been identified as a major source of ambient air fine particles in several European cities, where its relative contribution has been estimated to further increase in the future while PM emissions from other sources, such as industry and traffic, are decreasing (Denier Van Der Gon et al., 2015; Klimont et al., 2017). The amount and contents of the RWC emissions depend greatly on combustion conditions which

are generally affected by the combustion procedure, fuel, and appliance technology (Bhattu et al., 2019; Nuutinen et al., 2014; Orasche et al., 2013; Tissari et al., 2009). In logwood-fired appliances, there is also a strong variation in the emissions during the different combustion phases of batches, with ignition producing the highest organic emissions (Bhattu et al., 2019; Kortelainen et al., 2018). However, highest black carbon concentrations are emitted during the flaming phase, while the char burnout phase typically emits large amounts of carbon monoxide but low, mainly inorganic particulate emissions (Kortelainen et al., 2018). Combustion conditions also affect the emissions of many toxic compounds, such as polycyclic aromatic compounds (PACs) (Kim et al., 2013; Orasche et al., 2013), and are consequently strongly linked with the adverse health effects of the emissions (Bølling et al., 2009; Kanashova et al., 2018; Kasurinen et al., 2018).

Many of the main organic species in fresh, ~~unaged~~not atmospherically aged wood smoke are connected to the composition of wood fuel, such as levoglucosan, a common biomass burning marker, and lignin degradation products such as methoxyphenols and their derivatives (Elsasser et al., 2013; McDonald et al., 2000; Orasche et al., 2013). In addition, the gaseous organic emission from RWC contains ~~of~~ hundreds of ~~volatile~~ organic ~~species~~gaseous compounds (OGC) (Bhattu et al., 2019; Bruns et al., 2017; Hartikainen et al., 2018; Hatch et al., 2017; McDonald et al., 2000~~).~~), majority of which can be classified as volatile organic compounds (VOC) (Hatch et al. 2017), meaning that under ambient conditions they exist purely in gaseous phase. Notably, RWC is an important anthropogenic source for ~~volatile organic compounds (VOCs)~~OGCs with high potential for secondary particulate organic aerosol (SOA) formation. The most potent SOA-precursor compounds include aromatic hydrocarbons and oxygenated species, such as phenolic and furanoic compounds (Bruns et al., ~~2016; Hartikainen et al.,~~2016; Hartikainen et al., 2018) and removal of these compounds either via improved combustion conditions or for example catalytic cleaning have been shown to be efficient in lowering the SOA potential of RWC emissions (Czech et al., 2017; Pieber et al., 2018). Furthermore, the gaseous emissions contain high amounts of carbonyls, such as formaldehyde and acetaldehyde, with adverse health effects (Reda et al., 2015; U. S. EPA).

OA has an atmospheric lifetime of approximately one week (Hodzic et al., 2016), during which its chemical composition and potential environmental and health effects are likely to transform extensively. In daylight conditions, hydroxyl radicals (OH) dominate this aging process, where the oxidation of ~~VOCs and semi-VOCs~~OGCs forms a variety of functionalized products ~~with lower vapour pressures. These~~. Some of these oxidised secondary organic species partition into the particulate phase, resulting in an enhancement of ambient air particulate organic matter concentrations (Robinson et al., 2007). While aromatic ~~VOCs~~compounds are noted as the main SOA precursors from RWC, the complete pathway for SOA formation and the final SOA yields of complex ~~VOC~~OGC mixtures under different atmospheric conditions remain unclear (Bruns et al., 2016; Hartikainen et al., 2018; Hatch et al., 2017; McFiggans et al., 2019). Recent experiments on RWC exhaust estimate the mass of particulate OA to increase by a factor of 1.6–5.3 within approximately one day of photochemical aging (Bertrand et al., 2017; Bruns et al., ~~2015~~2015b; Grieshop et al., 2009; Heringa et al., 2011; Tiitta et al., 2016). In addition, ~~the photochemical transformation~~heterogeneous oxidation reactions of the particulate matter may be significant ~~when considering~~during the atmospheric ~~fate~~transformation of RWC emissions: it has been reported that only a minority of initial biomass burning particulate OA remains unreacted after a few hours of atmospheric aging (Hennigan et al., 2011; Tiitta et al., 2016). Photochemical aging also decomposes hydrocarbonaceous PACs (i.e., polycyclic aromatic hydrocarbons ~~(;~~ PAHs~~) in both the particulate and the gas phase,~~), which ~~may decrease the~~cause adverse health effects due to their carcinogenic properties ~~of the emissions or on~~. On the other hand, atmospheric aging may lead to ~~the~~ formation of even more toxic, oxygen- or nitrogen-substituted PACs (Keyte et al., 2013; Miersch

et al., 2019). For instance, these substituted PACs have been reported to cause a substantial part of the particle-induced mutagenicity in Beijing, with a contribution of only 8 % relative to the concentration of hydrocarbon PACs (Wang et al., 2011). Similarly, oxidation in nitrogen oxide (NO_x)-rich conditions can produce nitrophenols which are known to be harmful to ~~toward~~ plant growth and ~~for~~ human health (Harrison et al., 2005) and have been identified as an important constituent of light-absorbing organic matter ('brown carbon') (Moise et al., 2015; Zhang et al., 2011), thereby affecting atmospheric radiative forcing.

The photochemical aging of RWC emissions has previously been studied in smog chambers (Bertrand et al., 2017; Bruns et al., ~~2015~~2015a-b; Heringa et al., 2011; Tiitta et al., 2016), where the aging was monitored as a batch process from fresh emission to up to one atmospheric equivalent day of exposure (eqv.d) assuming an ambient average OH concentration of 10^6 molec cm^{-3}; Prinn et al., 2001). As an alternative, oxidation flow reactors (OFRs) with continuous sample flow have been increasingly utilised in combustion emission studies~~.~~ (Bruns et al., 2015a; Czech et al., 2017; Pieber et al., 2018). To achieve similar or higher oxidant exposures than chambers in shorter residence times, OFRs have been used with high ozone concentrations together with high-intensity low-wavelength UV lamps to generate OH-radical concentrations orders of magnitudes higher than those of smog chambers (Kang et al., 2007; Ihalainen et al., 2019; Simonen et al., 2017). Thus, OFRs enable measurements with better temporal resolution, which is a benefit when assessing the aging of aerosols from dynamic sources, such as batchwise logwood combustion.

In this study, we ~~investigated~~aim to determine how atmospheric aging changes the ~~photochemical transformation~~composition of organic aerosol, emitted by logwood fired stoves, as the ~~OA~~ function of OH-exposure. The atmospheric transformation of emissions from two RWC appliances fired with spruce and beech logwood~~. Atmospheric aging~~ was simulated using the photochemical emission aging flow tube reactor (PEAR~~) (~~ OFR; Ihalainen et al., 2019~~). In the PEAR, emissions were exposed~~) at different exposure levels ranging up to a ~~range of OH concentrations, after which the~~week of atmospheric age. The transformation of emissions and the formation of related secondary organic emissions were ~~measured~~monitored with a comprehensive ~~analysis~~ setup (Fig. 1~~). The OA measurements included~~), including analysis of gas-phase~~ analysis~~ by proton transfer reactor time-of-flight mass spectrometry (PTR-ToF-MS) and investigation of the particulate phase online by aerosol mass spectrometry (SP-HR-ToF-AMS) and offline by targeted gas chromatography mass spectrometry and thermal-optical analyses. ~~With photochemical exposure varying from 0 to 7 eqv.d, we assessed~~Together, these analyses enable the ~~transformation~~assessment of the OA chemical composition in both bulk and molecular level, from fresh emission to up to exposures representative of long-range transported smoke.

2 Material and methods

2.1 Experimental conditions

Experiments were conducted in the ILMARI laboratory of the University of Eastern Finland (www.uef.fi/ilmari) with the experimental setup shown in Figure 1. The two combustion appliances used were modern stoves with improved air intakes. First, a heat-storing masonry heater (Hiisi 4, Tulikivi Ltd., Finland) representing the typical modern logwood combustion technology utilised in Northern Europe, was fired with spruce logwood. The combustion procedure in the masonry heater consisted of three 2.5-kg batches (35-min combustion time) of spruce logwood representing kiln-dried fuel (5 % moisture content, S-5%), after which there was a 25-min char burning period prior to two 45-min batches with moist (22 % moisture content, S-22%) spruce logwood. Second, a non-heat retaining chimney stove (Aduro 9.3, Denmark) representing Middle-European modern logwood stoves was fired with both beech and spruce logs. The chimney stove

experiments consisted of five 2-kg batches (combustion time 40–55 min) of beech logwood (17% H_2O, B-17%), followed by two 50-min batches of S-22%. Beech was used in these experiments because it is the most common firewood used in Middle Europe, while spruce is used both in Northern and Middle Europe. For ignition, 150 g of dry kindling was placed on the top of the first batch in the cold furnace. Each batch was divided into three parts: ignition, flaming, and burnout phase. The ignition phase was determined to last from the beginning of the batch to the moment of batch maximum flue gas CO_2 concentration, and the burnout phase to begin from the moment when the CO concentration started to elevate and remained at a high level until the end of the batch (Fig. 2). The modified combustion efficiency (MCE) as a function of time was calculated from primary flue-gas CO_2 and CO concentrations as ΔCO_2 / (ΔCO_2 + ΔCO).

The exhaust was sampled from the stack with a 10 µm pre-cut cyclone. The sample was diluted with a combination of a porous tube diluter and an ejector diluter (Dekati FPS ejector, Finland) and had a dilution ratio (DR) of 40–150 (Table 1) when fed to the PEAR OFR. In the chimney stove experiments, an additional ejector diluter with a DR of 8 (Dekati DI-1000, Finland) was placed before the secondary online aerosol instruments. Compared to the no-aging experiments, a higher DR was selected for the aging experiments in response to the expected increase in particulate matter in the PEAR OFR during photochemical aging. Measured concentrations were corrected for the dilution and normalised to stoichiometric dry flue-gas by multiplication with the stoichiometric correction factor (SCF) of Eq. 1 based on the ~~secondary~~background CO_2 concentration ($CO_{2,bg}$), the CO_2 concentration in the diluted sample downstream the PEAR OFR ($CO_{2,sec}$), and the fact that the dry flue gas of wood combustion with no excess air contains 20.2 % CO_2.

$$SCF = \frac{20.2\,\% - CO_{2,background}}{CO_{2,sec} - CO_{2,background}} \frac{20.2\,\% - CO_{2,bg}}{CO_{2,sec} - CO_{2,bg}} \quad (1)$$

In addition, the secondary concentrations were normalised to a 13 % flue-gas oxygen content.

2.2 Use of the PEAR OFR

The PEAR OFR (Ihalainen et al., 2019) was used to continuously age the sample stream. In the setup, the extent of photon flux and consequential photochemical aging were controlled by adjusting the voltage of the 254-nm UV lamps. The total flow through the PEAR OFR was 60 L~~/~~ min~~-~~$^{-1}$ and the residence time within the PEAR 139 s . In addition to the 55 L~~/~~ min^{-1} sample flow, ~~additional~~ humified and purified air was introduced to the PEAR OFR to obtain a relative humidity of 45 ± 5 %. ~~In the aging experiments, 0.25–0.5 L/min ozone and 15 mL/min of butanol-*d9* were mixed with the main sample flow before the PEAR inlet (Fig. 1).~~ In the PEAR OFR, the photolysis of the ozone ~~formed~~forms hydroxyl radicals via reactions (2) and (3). Thus, the extent of photochemical aging in the PEAR ~~depended~~OFR depends on the photon flux inside the reactor and the introduction of OH precursors, namely, the externally fed O_3 and H_2O vapours.

$$O_3 + h\nu \rightarrow O_2 + O(^1D) \quad (2)$$

$$O(^1D) + H_2O \rightarrow 2\ OH \quad (3)$$

In the aging experiments, ozone and butanol-d9 mixed with the main sample flow before the reactor inlet (Fig. 1) resulted in concentrations of 2-11 ppm of O_3 (Table 1) and 80-200 ppb of butanol-d9 in the PEAR OFR before initiation of photochemical aging. The OH exposure (OH_{exp}) was determined continuously based on the butanol-d9 concentrations downstream the PEAR according to the method presented by Barmet et al. (2012~~) by introducing a constant flow of butanol-*d9* to the PEAR.~~). The OH_{exp} for clean air in the PEAR prior to the exhaust input ranged from 8.2×10^{10} to 1.6×10^{12} molec cm^{-3} s, which is equivalent to 1–18 days in an ambient atmosphere (eqv.d) with an estimated 24-hour average global OH concentration of 1×10^6 molec cm^{-3} (Prinn et al., 2005). The alternate reaction pathways in the PEAR OFR, namely, exposure to photolysis ($flux_{254nm,exp}$), excited ($O(^1D)_{exp}$), atomic oxygen ($O(^3P)_{exp}$), and ozone ($O_{3,exp}$), were assessed using the OFR exposure estimation equations of Peng et al. (2016) for OFRs with 254-nm lamps. Both the OH_{exp}

and the alternate reaction pathways were affected by the external OH reactivity (OHR_{ext}) (Li et al., 2015) of the gases in the sample fed to the PEAR OFR. The OHR_{ext} was calculated with Eq. (4) from the concentrations (c_i) of the primary gaseous compounds (Table S1) and the butanol-d9 in the PEAR OFR, with their OH reaction rate constants k_i ~~(Table S1).~~.

$$OHR_{ext} = \sum k_i c_i \quad (4)$$

Due to the differences in the emission concentrations during logwood combustion also the OHR_{ext} , and consequently OH_{exp}, vary also within a batch (Fig. S9). Average OHR_{ext} was in the range 130 – 1300 s^{-1} with the highest contributions from CO, NO, and unsaturated hydrocarbons (Fig. S5).

Particulate wall losses inside the PEAR OFR were minimised by conductive stainless-steel walls, laminar flow, and a relatively small surface-to-volume ratio (2.28 m^2:139 L) (Ihalainen et al., 2019). The particulate losses were estimated ~~by~~to be approximately 6 % based on the loss of elemental carbon (EC~~),~~) in the PEAR OFR, determined from the difference ~~between~~in the thermal-optical EC concentrations measured upstream and downstream of the ~~PEAR, whereas losses~~ reactor. The fate of the gaseous organic compounds capable of irreversible condensation under the present experimental conditions, i.e., low-volatility organic compounds (LVOC~~) were modelled~~), was estimated based on ~~the model of~~ Palm et al. (2016) by considering three possible depletion pathways: condensation onto particles, reactions with OH radicals, and condensation onto walls. To estimate the fraction of LVOC condensing onto particle phase, condensation sinks (Fig. ~~).~~S7) were calculated according to Lehtinen et al. (2003) using an average of the particle size distributions up- and downstream the PEAR OFR. See Section S2.2 for further information on LVOC fate estimation.

2.3 Offline filter sampling and analysis

PM_1 filter samples were collected on Teflon (PTFE, Pall Corporation, P/N R2PJO47) and quartz fibre (QF, Pall Corporation, Tissuquartz) filters simultaneously from primary and secondary exhaust at a 10- L~~/~~ min~~-1~~ flow rate, following the methodology presented by Sippula et al. (2009). A pre-impactor (Dekati PM-10 impactor) was used to separate the particles with aerodynamic diameters less than 1 µm (PM_1). For the masonry heater, samples were collected separately from the S-5% combustion (100-min collection time) and S-22% combustion (90-min collection time). From the chimney stove, two sample pairs were collected from the combustion of beech: full first two batches (85-min collection time), and fourth and fifth batches excluding the last 15 minutes (85-min collection time). The third chimney stove collection consisted of the combustion of two full batches of moist spruce (100-min collection time).

The Teflon filters were weighted before and after sample collection to determine the total PM_1 mass of the emission. The amount of organic (OC) and elemental carbon (EC) in PM_1 was determined from the QF filters by using a thermal-optical carbon analyser (Sunset Laboratory Inc.) following the protocol NIOSH5040 (NIOSH, 1999). In-situ derivatisation thermal desorption–gas chromatography–time-of-flight mass spectrometry (IDTD-GC-ToFMS) (Orasche et al., 2011), was applied ~~to the~~for targeted analysis of ~~semi-VOCs~~organic compounds in the particulate phase from the QF filters. Non-polar and polar compounds were identified and quantified using mixtures of ~~isotope~~isotopically labelled internal standards and calibration standards; see Supplementary Information Chapter S6 for further information of the analysis procedure. Majority of the targeted compounds can be classified as either semi- or intermediately volatile, meaning that under the present experimental conditions they can be partitioned into both gaseous and particulate phases.

2.4 Online ~~aerosol~~gas-phase measurements

Fourier transform infrared spectrometer (FTIR DX4000, Gasmet Technologies Inc.) was implemented on the stack to measure the amount of NO_x, CO_2, CO, and 27 ~~VOCs~~OGCs (Table S1) in the fresh exhaust. The measured primary ~~VOCs~~OGCs were grouped into four subgroups: alkanes, oxygenated compounds, and unsaturated and aromatic hydrocarbons. ~~After the PEAR, the~~The concentrations of CO_2, O_3, NO_x, and SO_2 were monitored at the outlet of the PEAR OFR with a trace-level single-gas analyzers (ABB CO_2 analyser, Siemens), and ~~organic gaseous compounds in the mass-to-charge (m/z) range of 40–180~~OGC were measured by PTR-ToF-MS (PTR-TOF 8000, Ionicon Analytik, Innsbruck, Austria), with H_3O^+ as the reagent ion and an electric field to gas number density ratio (E/N) of 130. Mass calibration was done with ~~-~~H_3O^+ (m/z 21.02) and 1,3-diiodobenzene (m/z 203.94), which was added as a calibrant for higher m/~~z~~z. The processing of the PTR-ToF-MS data was done in a manner similar to that of earlier work (Hartikainen et al., 2018). Reaction rates by Cappellin et al. (2012) were used when available; for other compounds, the reaction rate with H_3O^+ was assumed to be 2×10^9 cm^3 s^{-1} (Table S6).

2.5 Online particulate-phase measurements

Particle concentrations and mobility size distributions were monitored with scanning mobility particle sizers before (SMPS 3082, TSI, size range 14.6–661.2 nm) and after the PEAR OFR (SMPS 3080, TSI, size range 15.1–661.2 nm). An electrical low pressure impactor (ELPI 10 L~~/~~ min^{-1}, Dekati) measured the particle aerodynamic size distribution and the concentration of primary particles in the size range 18.6–5950 nm. The total particulate mass after PEAR OFR was measured with a tapered element oscillating microbalance monitor (TEOM, Model 1405, Thermo Scientific).

The composition of submicron particulate matter after PEAR OFR was measured by soot particle aerosol mass spectrometer (SP-HR-ToF-AMS, Aerodyne Research Inc). ~~The~~ The SP-HR-ToF-AMS dual vaporizer mode was used, with the combination of the thermal vaporizer (600 °C) and the continuous wave laser vaporizer (1064 nm) enabling the study of both nonrefractory (NR-PM) and refractory light-absorbing submicron aerosol particles (R-PM, e.g., refractory black carbon (rBC)) (Onasch et al., 2012). Standard mass-based calibrations were performed for the ionisation efficiency in the SP-HR-ToF-AMS using ammonium nitrate and Regal Black (Regal 400R Pigment Black, Cabot Corp.) particles (Jayne et al., 2000; Onasch et al., 2012). SP-HR-ToF-AMS was operated in V-mode from 12 to 555 m/z and the two vaporizer configurations were alternated every 120 s, including the particle time-of-flight (PTOF) mode (duration 20 s). The SP-HR-ToF-AMS data was analysed using the standard analysis tools SQUIRREL v1.62A and PIKA v1.22D adapted in Igor Pro 8 (Wavemetrics). The data was corrected by time-dependent background gas-phase CO_2 subtraction using the online HEPA filter measurement technique. The interactions of inorganic salts with pre-deposited carbon on the tungsten vaporizer was corrected according to Pieber et al. (2016). The CO_2-AMS interference calibration value was 0.3 % of the NO_3 concentration determined by NO_3NH_4 calibration and corrected via the fragmentation table according to Pieber et al. (2016). Before correction, the relative effect of the interference on O:C ratio was typically under 1 % and 5 % at maximum. The applied relative ionisation efficiency (RIE) was 1.4, which agrees with the OA mass concentrations of biomass-burning emissions within the stated ±38 % uncertainty of AMS (Bahreini et al., 2009; Xu et al. 2018). The elemental analysis of the OA was conducted using the Improved-Ambient method (Canagaratna et al., 2015), and the average carbon oxidation state (OS_C) of the OA was estimated as $OS_C \approx 2 \times$ O:C - H:C (Kroll et al., 2011).

The SP-HR-ToF-AMS OA mass spectra was further examined by positive matrix factorisation (PMF) using the method described in Lanz et al. (2007) and Ulbrich et al. (2009). Similar method have been used previously for example for the assessment of RWC generated POA and SOA in a chamber (Bruns et al., 2015a; Tiitta et al., 2016) and in an OFR

(Bruns et al., 2015a) or for time-resolved analysis of RWC OA emission constituents (Elsasser et al., 2013; Czech et al., 2016). The PMF Evaluation Tool v.3.05 was applied, and the standard data pre-treatment process was completed based on Ulbrich et al. (2009), including the application of minimum error criteria and down-weighting weak variables as well as m/z 44 (CO_2^+) and water-related peaks. The final four-factor PMF solution covered 98 % of the OA spectra (2.2 % residual). Additional factors did not increase the realistic physical meaning of the solution, while fewer factors were insufficient for a meaningful presentation of the data. The factor identification was confirmed by comparing the time series and mass spectra of each factor with external tracers (nitrate, sulphate, ammonium, chloride, PAH, CO_2^+, $C_2H_3O^+$, $C_4H_9^+$, and $C_2H_4O_2^+$). Furthermore, the factors were compared to logwood combustion mass spectra measured by Tiitta et al. (2016) from the aging of spruce logwood exhaust in a smog chamber. The agreement of spectra was denoted with both a coefficient of determination (R^2) and the angle between two mass spectra vectors (Kostenidou et al., 2009), where an angle less than 15° indicates a good agreement between two mass spectra.

The polycyclic aromatic hydrocarbons ~~(PAH)~~ and other ~~polycyclic aromatic compounds (~~PAC~~)~~ in the exhaust were analysed by using the PAC molecular ions as a proxy, following the P-MIP methodology presented by Herring et al. (2015). The base molecular ions $[M]^+$, their fragments ($[M\text{-}H]^+$ and $[M\text{-}2H]^+$) and isotopes (^2H, ^{13}C, $^{13}C_2$, ^{15}N, ^{17}O, and ^{18}O) were isolated and quantified using the SP-HR-ToF-AMS high-resolution analysis software tool (version 1.22D). The targeted ions included those previously connected with PACs (Herring et al., 2015) and compounds typically released from ~~residential wood combustion~~RWC (Avagyan et al., 2016; Bertrand et al., 2018; Bruns et al., ~~2015~~2015b; Czech et al., 2018; Miersch et al., 2019). The 61 PACs considered (Table S8) were separated into five subgroups: unsubstituted PAHs (UnSubPAHs), oxygenated ~~PAHs~~PACs (OPAHs), methylated ~~PAHs~~PACs (MPAH), nitrogen-substituted ~~PAHs~~PACs (NPAHs), and amino ~~PAHs~~-PACs (APAHs). See Supplementary Information Chapter S5 for further information on SP-HR-ToF-AMS analyses.

3 Results and ~~conclusions~~discussion

This study comprehensively characterises the chemical properties of RWC exhaust at different atmospheric aging times by combining extensive information gathered from gas-phase and particulate phase chemical analyses. In this section, we first discuss the dynamic combustion conditions and the characteristics of primary emissions from logwood stoves utilized with different fuels, which define the starting point for the aging experiments. Next, the aging conditions in the PEAR OFR are evaluated in order to validate the atmospheric relevance of the results. Finally, we assess the changes in the gaseous and particulate OA during the aging process under a variety of different oxidant concentrations. The observations of changes both in bulk- and molecular level aerosol chemical composition demonstrate that the major transformation pathway of OA changes from initial gas phase functionalisation followed by condensation to the transformation of the particulate OA by heterogeneous oxidation reactions and fragmentation. The study shows a linear dependency between OH exposure and organic aerosol oxidation state. Furthermore, OH-exposure-dependencies of specific OA constituents, such as nitrophenols, carboxylic acids and PACs, are established.

3.1 Combustion conditions

The average modified combustion efficiency was greater than 0.97 for the masonry heater and greater than 0.95 for the chimney stove, with lower MCE occurring mainly during the char burnout periods (Fig. S1). These values are typical for modern batch-wise operated logwood appliances (Bhattu et al., 2019; Czech et al., 2018; Heringa et al., 2011). In addition to the variation within a combustion batch, there were also differences between the individual batches (Fig. 2). Notably,

the combustion conditions during the first batch were distinct from later batches~~. This was a result~~, because of the ~~lower initial temperature which~~ignition in a cold firebox. This caused a longer ignition period (determined by the rising CO_2 concentrations), which lasted for 24 ± 5 % (masonry heater) and 35 ± 4 % (chimney stove) of the total duration of the batch~~;~~, whereas in the later batches~~,~~ the firebox temperatures are higher ~~initial temperature shortened~~ and the ignition shortened to 9 ± 3 % (masonry heater) or 8 ± 4 % (chimney stove) of the total combustion time. Furthermore, the flaming phases of the first batches were shorter than those of the following batches of dry spruce or beech fuels. The emission profiles were affected by these batchwise differences, with ignition being the period for enhanced organic emissions, whereas the flaming phase was characterized by an increase in particulate emissions consisting mainly of black carbon, as expected based on previous work (Kortelainen et al., 2018). The char burnout phases with these fuels were characterised by high CO concentrations, whereas in moist spruce combustion elevated CO concentrations were measured throughout the batch, thus making the burnout phases less distinguishable.

3.2 Primary emissions

3.2.1 Gaseous organic emissions

The primary organic gaseous emissions in the undiluted flue gas were measured ~~constantly~~continuously by an FTIR multicomponent analyser~~ from the undiluted flue gas~~. Additionally, the PTR-ToF-MS measured diluted, unaged emissions during the no-aging experiments. These datasets complemented each other because, while FTIR ~~measured only~~ was calibrated for 27 typical combustion-derived ~~VOC~~compounds (Table S1), a more detailed insight of the ~~VOC~~ composition of the gaseous organic phase was acquired via the PTR-ToF-MS ~~detection of 127~~, with which 126 different molecular formulas for ~~gaseous species~~OGC in the primary ~~aerosol~~emissions were identified in the m/z range of 40–180 (Table S6). However, PTR-ToF-MS is unable to detect ~~for example~~ compounds with proton affinities lower than that of water (691 kJ mol^{-1}), such as alkanes~~ because of their low protonation efficiency.~~. Furthermore, ~~the~~ fragmentation ~~of~~in the ~~-~~PTR-ToF-MS ~~limited in~~limits the ~~quantification~~identification of compounds with similar mass-to-charge ratios as ~~those of~~ common fragment ions, including unsaturated aliphatic compounds, such as propene ($C_3H_6^+$) at m/z 41.04 or butene ($C_4H_8^+$) at m/z 57.08~~; however~~. However, these compounds were detected ~~using~~by the FTIR.

The major ~~VOC~~OGC groups measured by PTR-ToF-MS were carbonyls, aromatic hydrocarbons~~,~~ (ArHC), furans, and phenols (Fig. ~~6~~4; Table S2). In addition, unsaturated aliphatic compounds constituted a substantial fraction of ~~VOC, as~~the total non-methane OGC (NM-OGC) measured using the FTIR (Fig. 3). The ~~total VOC~~NM-OGC emissions based on FTIR were 42.6 ± 9~~ ± 10.5~~.2 and ~~102 ± 28.0~~101 ± 24.6 mgC m^{-3} for dry and moist spruce combustion in the masonry heater, respectively, and 89.~~0 ± 13.5~~4 ± 11.3 and ~~147 ± 24.9~~148.3 ± 23.0 mgC m^{-3} for beech and moist spruce in the chimney stove, respectively. Thus, the lowest ~~VOC~~NM-OGC concentrations were measured from the dry spruce combustion. Moist spruce combustion produced a factor of 1.7–3.6 higher emission than dry wood, which is well in line with studies by e.g. McDonald et al. (2000), where moist fuel produced 2–4 times more ~~VOC~~NM-OGC than dry fuel combustion. The difference between concentrations was highest for oxygenated compounds (factor of 4.2~~±~~ ± 1.7) and for unsaturated compounds (2.7±0.6), but statistically significant for all subgroups (paired t-test p-values ≤0.02 for all groups for the consecutive dry/moist experiments; Table S2). Differences in ~~VOC~~NM-OGC emissions were also observed between the masonry heater and the chimney stove. Emissions from moist spruce combusted in the chimney stove were higher by a factor of 1.5 (p-value 0.05) compared to the masonry heater, with a significant increase in unsaturated and aromatic hydrocarbons (factors of 1.6 and 1.7, respectively, p-values <0.01) based on FTIR measurements.

The ~~VOC~~NM-OGC emissions of the first batches exhibited a distinct time-dependent behaviour in comparison to the following batches~~; i.e.,~~; the emitted concentrations always increased both after ignition and at the end of flaming phase (Fig. 2), whereas in the following batches there was a sharp emission peak at ignition, after which the concentrations declined as soon as the flaming phase began. These findings agree with those by Kortelainen et al. (2018) and are influenced by the fact that cold ignition is performed from the top of a fuel batch, while the following batches are ignited from the bottom by the glowing embers. ~~VOC~~NM-OGC emissions were lowest during the burnout period when most of the fuel was already consumed (Fig. ~~S2~~2). Thus, ~~VOC~~NM-OGC emissions have a reverse time profile to the CO emissions, which peak during the char burnout phase. Furthermore, the contribution of the different organic compound groups to the total ~~VOC~~NM-OGC concentration differed in relation to time (Fig. ~~S3~~3, Fig. S2). For example, the importance of aromatic species increased for dry fuels (S-5% and B-17%) for the flaming and burnout phases, while other species were pronouncedly emitted at ignition. In addition, the composition of aromatic species measured with PTR-ToF-MS in the unaged emission depended on the phase (Fig. ~~S4~~S3). In the masonry heater, ~~aromatic hydrocarbons (~~ArHC~~)~~ had ~~a~~the highest contribution during the ignition phase, but their relative share decreased during flaming phase, while the share of furanoic and phenolic compounds increased. The relative importance of furanoic and phenolic compounds in the fresh exhaust of the flaming phase from a masonry heater has been also previously established (Czech et al. 2016). Overall, the share of ArHC in the fresh exhaust is higher and less phase-dependent for beech combustion in chimney stove than for other experiments. The share of N-containing aromatic compounds, namely, nitrophenol and -cresol, also increased after ignition. These findings are important also when considering the potential of SOA formation, as aromatic ~~VOCs~~compounds have been observed to be the major SOA precursors in RWC emissions, and removal of ArHC from the flue gas either by improving combustion conditions or using e.g. catalytic cleaning has been noted to decrease also the resulting SOA formation (Bruns et al., 2016; Hartikainen et al., 2018; Pieber et al., 2018).

3.2.2 Particulate emissions

The average primary PM_1 mass ~~emissions ranging from~~concentrations, 33 ~~to~~– 67 mg m^{-3}, and the number ~~emissions from~~concentrations, 3.2×10^7 cm^{-3} ~~to~~– 5.4×10^7 cm^{-3} (Table 2~~)~~), were on a similar level with earlier studies reporting emissions from modern logwood stoves (Kortelainen et al., 2018; Nuutinen et al., 2014; Tissari et al., 2009). The combustion of dry spruce in a masonry heater emitted 1.5- and 2 -fold PM_1 mass compared to that of moist spruce and beech, respectively, mainly because of the higher elemental carbon emissions. Moist spruce generated similar PM_1 emissions with both combustion appliances. The organic carbon to elemental carbon ratio (OC:EC) of dry spruce combustion was very low (0.07 ± 0.02, Table 2) compared to that of moist spruce combustion (0.31 ± 0.45 for masonry heater and 0.25 ± 0.04 for chimney stove) and beech combustion (0.15 ± 0.04). Such low OC:EC ratios have been previously reported for emissions from modern masonry heaters operating with dry logwood (Czech et al., 2018; Miersch et al., 2019; Nuutinen et al., 2014).

The particle size distribution (~~Figs. 4 and S5~~Fig. S4) from dry spruce combustion was clearly distinguishable from that of other wood fuels and showed considerably larger mean particle mobility size (GMD 95.5 nm) compared to those of other fuels (GMD 52.8–68.4 nm). The soot-dominated composition of S-5% exhaust likely increases the GMD, because soot particles are typically present as larger agglomerates than particles of inorganic origin (ash) which mainly form ultrafine particles (Tissari et al., 2008). The size distribution and number concentration of particles in an exhaust are not only important because of their link to potential health effects, but also during aging of the exhaust, because they affect the condensation sink (CS) (Lehtinen et al., 2003) of condensable vapours during the dilution and aging process.

Thus, the particle number concentrations and size distributions affect the fate of condensable vapours and the overall OA enhancement ratios. ~~The fates of low-volatility condensable vapours are further discussed in the chapter 3.3.1.~~

The thermal-optically measured elemental carbon in both the primary and the secondary exhausts correlated well with the refractory black carbon (rBC) measured by SP-HR-ToF-AMS from the secondary exhaust (R^2 = 0.74 and 0.76, respectively; see Fig. ~~S14~~S15). Analogous to the elemental carbon results, rBC emission was highest during the combustion of kiln-dried spruce (49.3 ± 13.7 mg m^{-3}). Dry fuel has recently been found to increase the soot and PAC emissions also for combustion of birch logwood in sauna stoves (Tissari et al., 2019). Considering the different combustion phases, rBC emissions were highest during high-temperature, flaming combustion as previously noted also by e.g. Kortelainen et al. (2018). For moist spruce, the rBC concentration dropped to 24.8 ± 12.3 mg m^{-3}, likely because of the lower temperature and consequentially slower burn rate. Similar rBC concentrations (24.0 ± 6.0 mg m^{-3}) were also measured from spruce combustion in the chimney stove. Unlike the masonry heater where the rBC concentrations were similar throughout the three dry batches, the rBC concentration from the combustion of beech in a chimney stove decreased considerably after the first batch, from 57.7 ± 7.2 mg m^{-3} to 15.6 ± 5.2 mg m^{-3}. While aging had no effect on the rBC mass, it plays an important role in the formation of SOA by acting as a seed for condensation during aging. Furthermore, soot cores composed of elemental carbon are chemically active and may enhance the photooxidation of an OA condensed onto soot agglomerates through electron transfer (Li et al., 2018).

3.3 OFR conditions

~~3.3.1 Wall losses and fate of condensable vapours~~

~~The loss of primary particles in the PEAR was estimated at 6 % based on the thermal–optical measurements of elemental carbon. When estimating the fate of the LVOC in the PEAR, three possible depletion pathways were considered: condensation onto particles, reactions with OH radicals, and condensation onto walls (Palm et al., 2016). To estimate the fraction of LVOC condensing onto particle phase, condensation sinks (Fig. 4) were calculated according to Lehtinen et al. (2003) using an average of the particle size distribution before and after PEAR. Similar to earlier studies, the downstream particle number concentration and condensation sinks were influenced by new particle formation (Fig. S13) with the extent of nucleation depending strongly on the aging conditions (Bruns et al., 2015; Ihalainen et al., 2019; Simonen et al., 2017). Long aging conditions greater than 4 eqv.d led to particularly strong increase in the amount of sub-50 nm particles. The new particle formation occurred mainly during the periods when the concentrations of condensable vapours were high; that is, most notably during the ignition phase. However, the distinct formation of ultrafine particles does not necessarily represent the atmospheric fate of condensable vapours because of the faster than ambient oxidation resulting in faster gas to particle conversion and higher saturation ratios in the PEAR. At lower OH exposures, the condensation growth was mainly observed as an increase in the number concentration in the larger size range, while less nucleation to new particles was observed than that in long aging experiments.~~

~~The importance of different LVOC fates is shown in Figure 5. The majority of the LVOCs condensed onto the particles, and a portion also depleted by reactions with oxidants in the PEAR, while the LVOC wall losses were primarily below 2 %. The amount of LVOCs estimated to exit the PEAR as gas phase LVOCs exceeded 0.1 % only during the middle burnout phase of the masonry heater combustion because of the low particle number concentrations during the char burning phase between the change from dry spruce to moist spruce combustion, which generated a low condensation sink into the PEAR.~~

~~3.3.2 Photochemical aging conditions~~

During photochemical aging, ~~external OH reactivity (~~OHR_{ext}~~)~~ is an important parameter affecting OH-radical consumption and reaction pathways of organic species. For the masonry heater experiments, the average OHR_{ext} was ~~98–107~~130–150 s^{-1} for dry spruce samples and ~~125–172~~160–220 s^{-1} for moist spruce. In the chimney stove, the average OHR_{ext} was ~~237–252~~280–300 s^{-1} for beech and ~~278–308~~320–370 s^{-1} for moist spruce samples, except for the low-DR experiment (Exp. 5, DR of 30) where the average OHR_{ext} reached ~~684~~820 and ~~1110~~1300 s^{-1} for the beech and moist spruce samples, respectively. The OFR conditions were divided into good, risky, and bad based on the ratio of the photon flux exposure to OH_{exp} by the definitions of Peng and Jimenez (2017) (Fig. ~~S7~~S6). Here, the aging conditions were defined as mainly "risky" (4×10^5 cm s^{-1} < $flux_{254nm,exp}/OH_{exp}$ < 10^7 cm s^{-1}) during all the experiments. The OHR_{ext} varied considerably during combustion cycles, but the limit for ~~bad~~'bad' conditions was exceeded ~~briefly (up to 7 % of total experiment time)~~ only ~~in a few experiments~~ during ignition phases of chimney stove experiments when the OHR_{ext} peaks above 1000 s^{-1}~~.~~ for brief periods accounting for up to 4 % of total experiment time. In terms of OA emission, the ~~limit for bad conditions was exceeded in one masonry heater experiment (S-22%, Exp. 5), where 4 % of OA mass was emitted during this period. For the chimney stove experiments,~~ bad conditions accounted for ~~2–9~~3–7 % of chimney stove OA emissions, excluding the S-22% combustion for the low-DR experiment ~~(46~~where 30 % of OA was emitted under 'bad' conditions~~).~~.

~~The~~Evaluation of the OHR_{ext} ~~calculations were~~was limited to the externally added butanol-d9 and the compounds measured from the primary exhaust with FTIR, with NO, CO, and unsaturated hydrocarbons as the main OHR_{ext} producers (Fig. ~~S6~~S3). In other words, the products of later-generation oxidation or from fragmentation from the particulate phase were not considered. ~~In addition, the prevailing~~ The average NO_x concentrations input to the PEAR OFR ranged ~~on average~~ from 150 to 420 ppb, except for the low-DR experiment ~~at a concentration~~with concentrations of 1140 and 751 ppb for beech and spruce combustion, respectively. NO is rapidly oxidized to NO_2 with the addition of O_3 and then partially converted to particulate nitrate~~, and the~~. The subsequent low-NO conditions in the PEAR ~~reduced~~decreased the reactions of organic peroxy radicals (RO_2) with NO. Based on the RO_2 chemistry model by Peng et al. (2019) for 254 nm OFRs, the high photon fluxes and high concentrations of both OH and HO_2 in the PEAR OFR result in lower RO_2 lifetime and consequently lower RO_2 isomerization rate than in atmosphere, while the importance of RO_2+OH reaction is enhanced due to lower-than-ambient HO_2-to-OH-ratio (Peng et al. 2019).

The average batchwise OH exposure in the PEAR OFR during photochemical aging experiments ranged from 0.5 to 7 eqv.d depending on the applied photon flux and the OHR_{ext} of the sample. During the experiments, the photochemical exposure varied in line with the varying OHR_{ext} during batchwise combustion, with the highest exposure occurring during the flaming phase and lower exposure during the ignition period (Fig. ~~S8~~S9). The extent of alternative non-OH reaction pathways during photochemical aging in the PEAR OFR were compared to the tropospheric conditions (Chapter S2.3), and the exposures to $O(^1D)$ and $O(^3P)$ in the PEAR OFR were ~~shown~~estimated to be similar to those in ambient conditions (Fig. ~~S9~~S10), excluding the ignition period during the low-DR experiment, where the importance of $O(^3P)_{exp}$ briefly exceeded ambient conditions. However, the exposure to ozone in relation to OH radicals was estimated to be lower in the PEAR OFR than in the troposphere ($O_{3,exp}/OH_{exp}$<10^5~~), thus leading to more OH-dominated chemical reactions when only considering the initial O_3 input.~~). However, our estimations were based on the initial O_3 concentrations, whereas O_3 is expected to form in the PEAR OFR during photochemical aging ~~because it is~~as a product of the OH + ~~VOC~~OGC reactions (Carter, 1994). This may have led to the $O_{3,exp}/OH_{exp}$ being slightly underestimated.

Several of the emitted ~~VOCs~~OGCs were susceptible to photolysis at 254 nm, most importantly the ~~aromatic hydrocarbons~~ArHC, which are among the main SOA precursors from RWC. Photolysis as a degradation pathway can exceed OH reactions also in the atmosphere for compounds with high photolysis rates (Hodzic et al., 2015). Here, the importance of photolysis was notable for e.g. benzene, of which more than 40 % may have degraded via photolysis (Fig. ~~S10~~S11). However, the importance of photolysis during photochemical aging is inversely proportional to the ratio of the OH reaction rate to the photoabsorption cross section (σ_{abs}), and it can be considered a minor pathway for other main ~~VOC species~~OGCs (Table S5), including other aromatic species such as toluene (<10 % of total degradation during these experiments~~, see~~; Fig. ~~S10).~~ S11).

The detailed results of the LVOC fate calculations are presented in the section S2.2. Briefly, the majority of LVOCs were estimated to condense into the particulate phase in all experimental conditions (Fig. S8). Similar to earlier OFR studies (Bruns et al., 2015a; Ihalainen et al., 2019; Simonen et al., 2017), the downstream particle number concentration and condensation sinks were influenced by new particle formation (Fig. S14) with the extent of nucleation depending strongly on the aging conditions and the concentrations of condensable vapours. However, the distinct formation of ultrafine particles does not necessarily represent the atmospheric fate of condensable vapours because of the faster-than-ambient oxidation, which results in higher saturation ratios and faster gas-to-particle conversion in the PEAR. Gas-to-particle conversion is also affected by the dilution ratio, which was in the PEAR OFR lower than what typically exists in atmosphere. Therefore, it has to be noted that the relative fraction of the measured semivolatile species in the condensed phase are likely lower at ambient dilution ratios than in the OFR experiments of this study.

3.4 Transformation of gaseous phase

The composition of the ~~VOCs~~OGCs changed throughout the studied exposure range, and the abundance of the secondary ~~VOCs~~compounds increased with an increase in photochemical exposure. However, while the small oxidised organics became increasingly dominant in the gas phase, photochemical aging particularly decreased the share of aromatic compounds (Fig. ~~6~~4). Namely, the ~~VOCs~~OGCs measured with PTR-ToF-MS from the aged gas phase were governed by small carbonyls and fragmentation products such as acetic acid ($C_2H_4O_2$, m/z 61.02). The evolution of the total chemical composition is visualised in the van Krevelen -diagram, which is often used for simplified characterisation of particulate OA (Heald et al., 2010) and was here extended for the investigation of the gaseous organic phase measured by PTR-ToF-MS (Fig. ~~7~~5). Photochemical aging caused several simultaneous and subsequent functionalisation reactions of the organic compounds, and the increase in the average H:C ratio together with an increasing O:C ratio led to linear slopes from +0.69 to +1.0 in the van Krevelen diagram. Similar, positive slopes are derivable also from previous studies of aging of RWC OGC in smog chambers (Bruns et al., 2017; Hartikainen et al., 2018). Most of the ~~VOCs~~OGCs in primary RWC exhaust have relatively high OH reactivities (Fig. ~~S11~~S12), and thus their reactions are expected to take place within the first atmosphere equivalent hours of photochemical aging (Bruns et al., 2017; Hartikainen et al., 2018). ~~This indicates the continuous contribution from~~Therefore the secondary OGC products, including the oxidised fragmentation products from the particulate phase, dominate the total OGC in the long-range transported smoke. In addition, the loss of compounds with low H:C and O:C ratios, such as aromatic species, is important for the change of the average composition. Furthermore, the oxidation of compounds undetected by the PTR-ToF-MS, such as alkanes, may introduce secondary products with higher proton affinities and their ~~consequent~~subsequent appearance in the spectra. Conversely, aging may also lead to the growth of compounds outside the ~~considered~~observable mass range (m/z 40–180). Compared to previously measured changes of RWC exhaust in a chamber (Hartikainen et al., 2018), aging in the PEAR OFR led to a slightly

higher increase in the H:C ratio. This difference implies an increased fragmentation which is likely the result of faster ~~aging process~~OH exposure and differences in the RO_2 chemistry (Peng et al., 2019) in the PEAR OFR compared to that in a smog chamber.

Aromatic compounds consisting of ~~aromatic hydrocarbons (~~ArHCs~~),~~, phenols, furans, N-containing aromatic compounds (N-aromatics), and other oxygenated aromatics were important constituents of the primary organic gas phase and formed 37–39 % of the fresh ~~VOCs~~emission from the masonry heater and 33–34 % from the chimney stove, as measured by the PTR-MS-TOF (Fig. ~~9~~4). Similar shares have been measured from fresh RWC exhaust by Bruns et al. (2017) (13–33 %) and Hartikainen et al. (2018) (33 –36 %). However, after 2 eqv.d of exposure, their share decreased to less than 20 % of the identified ~~VOCs~~OGCs, which agrees with previously reported conversions of aromatics during photochemical exposure (Bruns et al., 2017; Hartikainen et al., 2018). Overall, the photochemical reactions of aromatics are an important source of SOA because they form products that efficiently partition into the particulate phase. However, there are large differences between the conversion efficiencies of aromatic compound groups. While ArHCs comprise approximately half of the aromatic ~~VOCs~~compounds in fresh gaseous exhaust, their share grows to over 70 % in 5–7 eqv.d, while the share of oxygenated aromatics decreases with aging in line with their higher OH reactivity. Similar aromatic behaviour in RWC exhaust was observed earlier in a chamber with spruce exhaust (Hartikainen et al., 2018), where the molar share of ArHCs in the total aromatic content increased from 45 % and 32 % to 63 % and 54 % during aging of 0.6 and 0.8 eqv.d, respectively, while the share of furanoic and phenolic species decreased. Furthermore, N-aromatics were not detectable here with ages exceeding 1 eqv.d, although they have been observed to form with shorter exposures (Hartikainen et al., 2018). The N-aromatics produced by the first stages of aging may have partitioned to the particulate phase but are also degraded by subsequent reactions with OH. Simultaneously, the share of aliphatic nitrogen compounds (CHN and CHNO) to the total concentration ~~remained relatively stable.~~was not substantially affected by photochemical exposure.

Carbonyls were divided into primary and secondary subgroups based on their behaviour during aging (Table S6). The primary carbonyl group, consisting mainly of acetaldehyde and to a smaller extent of compounds such as acrolein and butadiene, was prevalent in the fresh exhaust, but their share of identified compounds decreased from 13–27 % in unaged exhaust to 3–12 % in the highest exposures. This is the result of both the degradation of these compounds and the introduction of high amounts of carbonyls in the secondary carbonyl group. The ratio between the two carbonyl groups increased linearly with age (Fig. ~~S12~~S13). The secondary carbonyl group was dominated by acetic acid, which was the most prevalent compound after extensive aging in all experiments and covered over 30 % of the total measured ~~VOC~~OGC concentration from the highly aged S-5% and B-17% exhaust. The mainly small acidic compounds in the secondary carbonyl group were formed from the photochemical reactions of ~~VOCs~~OGCs and from particulate OA, which is a consistent source of oxygenated ~~VOCs~~OGCs such as acetic acid, formic acid, acetaldehyde, and acetone (Malecha and Nizkorodov, 2016). Of these, acetaldehyde is classified as a primary carbonyl because it reacts with OH two orders of magnitude faster than the ~~others~~other considered small carbonyls (Atkinson et al., 2001), and thus its concentration remains ~~stable~~at a similar level throughout the aging process.

3.5 Transformation of particulate phase

3.5.1 OA enhancement and composition

The photochemical aging process increased the mass of particulate organic carbon measured with thermal–optical carbon analysis by factors of 1.3 and 3.9 for dry and moist spruce combustion in a masonry heater, respectively, and by factors

of 2.0 and 3.0 for beech and moist spruce combustion in a chimney stove, respectively. This agrees well with the previously observed SP-HR-ToF-AMS-based OA enhancement factors (1.6–5.3) for RWC (Bertrand et al., 2017; Bruns et al., 20152015b; Grieshop et al., 2009; Heringa et al., 2011; Tiitta et al., 2016) and with the thermal-optical analysis-based organic carbon enhancements previously measured for the same chimney stove (1.3–1.4 after 1.7–2.5 eqv.d) (Miersch et al., 2019). The organic carbon concentrations after the PEAR OFR correlated well with the OA measured with SP-HR-ToF-AMS (R^2 = 0.85, Fig. S14S15). Aging led to a linear increase in the SP-HR-ToF-AMS-derived ratio of organic matter to organic carbon (OM:OC, Fig. S16S17), which rose from the initial average ratio of 1.8–2.2 to 2.7–3.0 during extended aging. Similarly, the OS_C of the OA increased as a function of the photochemical age throughout the tested exposure ranges (Fig. S16S17), indicating the existence of continuing reactions of the particulate phase after the rapid consumption of the majority of the primary gaseous SOA precursors with relatively high OH reaction rates (Fig. S11). In contrast, asS12). As expected, the organic carbon mass enhancement did not increase with continuous aging because the major SOA precursors were already consumed by relatively short OH exposures. Continuing photochemical exposure may instead reduce the amount of particulate organic carbon (Kroll et al., 2015), which acts as a source for volatile acidic compounds during photochemical aging (Malecha and Nizkorodov, 2016; Paulot et al., 2011). See Table S7 for experiment-wise average concentrations and oxidation states.

The oxidation states measured after the PEAR OFR without oxidative aging were highest for the chimney stove OA, with average unaged OS_Cs of 0.22 and 0.41 for beech and spruce combustion, respectively, while dry and moist spruce in the masonry heater had average unaged OS_Cs of -0.18 and 0.15, respectively. This indicates the existence of different combustion conditions in the studied appliances, with the masonry heater having lower emissions of highly oxygenated compounds and a higher share of unsaturated hydrocarbons compared to that of the chimney stove emissions. However, as a result of oxidative aging, OS_C surpassed 1.5 after 5 eqv.d regardless of the type of experiment. , which exceeds the values typically observed in ambient aerosol (Kroll et al. 2011, Ng et al. 2011). This isA higher initial oxidation state in the chimney stove exhaust led to shallower slopes (-0.17 and -0.34) in the van Krevelen diagram than those in the masonry heater exhaust (-0.46 and -0.49, Fig. 8). Previously, the aging of spruce combustion exhaust from a masonry heater in a chamber has produced similar but slightly steeper van Krevelen slopes of -0.64 – -0.67 (Tiitta et al., 2016). The steepness may be affected by the lower aging and consequent lower final OS_C (maximum of +0.14) as the O:C ratio has been noted to level off at higher oxidation states (Ng et al., 2011). Slopes are also positively affected by fragmentation which may be enhanced in the PEAR because of the more intensive UV radiation than in smog chambers or in ambient conditions. The OS_C of highly aged exhaust exceeds that observed in ambient aerosol (Kroll et al. 2011, Ng et al. 2011), likely because highly aged aerosol in ambient air is mixed continuously with fresh and less oxidised sources. However, the chemical evolution of OA in the PEAR did followOFR followed a similar trend to that observed for typical ambient semi-volatile oxygenated aerosol which had, with a van Krevelen slope of -0.5 pointing to e.g., which can be interpreted as a result of simultaneous fragmentation and acid-group addition (Ng et al., 2011). Furthermore, the changes in OS_Cs were similar to those previously observed for ambient aerosol aged extensively in ana potential aerosol mass (PAM; Kang et al., 2007) OFR (OS_C up to 2, Ortega et al., 2016), and the van Krevelen slopes agreed well with those previously measured from single precursors). The OS_Cs of RWC exhaust aged in an oxidation reactor, such as -0.48 for toluene or -0.46 for xylene (Lambe et al., 2011a PAM OFR have, however, been notably lower than observed here (Fig. 6; Bruns et al., 2015a; Pieber et al., 2018).

A higher initial oxidation state in the chimney stove exhaust led to shallower slopes (-0.17 and -0.34) in the van Krevelen diagram than those in the masonry heater exhaust (-0.46 and -0.49, Fig. 6). The slope for the beech combustion

aerosol was higher than for spruce, which may result from differences in fuel composition as has been observed also previously for biomass burning OA (Ortega et al. 2013). Previously, the aging of spruce combustion exhaust from a masonry heater in a chamber has produced similar but slightly steeper van Krevelen slopes of -0.64 – -0.67 (Tiitta et al., 2016). The steepness may be affected by the shorter aging (< 1 eqv.d) and consequent lower final OS_C (maximum of +0.14) in the chamber, as the O:C ratio has been noted to level off at higher oxidation states (Ng et al., 2011). Slopes are also positively affected by fragmentation which may be enhanced in the PEAR OFR because of the more intensive UV radiation than in smog chambers or in ambient conditions. The van Krevelen slopes agreed well with those previously measured from single precursors aged in the PAM OFR, such as -0.48 for toluene or -0.46 for xylene (Lambe et al., 2011). Similar slopes have been observed also for aging of OA from pellet combustion (-0.47 – -0.44; Czech et al. 2017) or open biomass combustion (-0.5; Ortega et al. 2013) with a PAM OFR.

The evolution of particulate organic aerosol was assessed also by the IDTD-GC-ToFMS analysis of filter samples. When comparing the concentrations in the exhaust after the PEAR OFR, the concentrations of compounds with high oxidation states and low number of carbons (n_C) increased during photochemical aging (upper-right corner of Fig. ~~10~~7). The locations of the measured organic compounds in the OS_C:n_C space are shown in Figure ~~S19~~S20, and their dilution-corrected concentrations downstream the PEAR OFR in Table S12. In the OS_C:n_C space, the compounds which exhibited a major increase during photochemical aging were located in or above the location of the low-volatility oxidised organic aerosol (LV-OOA) classified by Kroll et al. (2011). These compounds are products of the multistep oxidation process including both fragmentation and oxidative reactions.

OA formation is tied to the availability of organic precursors, and thus the formation of SOA was highest at the ignition phase of each batch (Fig. ~~S15~~S16). In the masonry heater, the aged particulate OA mass increased considerably with the introduction of moist logs, simultaneously with the increase in gaseous organics in the fresh emissions. In contrast, the low organic emission by dry spruce combustion was reflected as a lower SOA formation. Another aspect related to the primary exhaust was the extent of OH exposure in the PEAR OFR, which was directly connected to the sample concentrations, as discussed in Chapter 3.3.~~2; namely~~ Namely, the photochemical aging was lower during periods of high emission, leading to lower oxidation states for the OA emitted during ignition.

3.5.2 PMF analysis of particulate OA composition

PMF analysis applied to the exhaust produced a four-factor solution for the OA covering 98 % of the spectra. The spectra of the factors are shown in Figure ~~S17~~S18. Two of the factors were associated in particular with the primary OA from biomass combustion: pyrolysis-BBOA, formed especially during ignition, and flaming-BBOA, emitted pronouncedly during the flaming phase. The other two factors, semi-volatile oxygenated OA (SV-OOA) and low-volatility oxygenated OA (LV-OOA), represent oxygenated organics with notably higher OS_Cs than those of the primary OA factors (Table 3). Flaming-BBOA comprised 76 % and 55 % of the unaged OA from dry and moist spruce combustion in the masonry heater, respectively, but only 27 % and 23 % in the beech and moist spruce combustion OA from the chimney stove, respectively (Fig. ~~10~~8), indicating a less-oxidising higher-temperature flaming phase in the modern masonry heater. Flaming-BBOA is strongly related to the $C_4H_9^+$ -ion (main peak of m/z 57, R^2 = 0.90, Fig. ~~S18)~~S19), which is used as a tracer for hydrocarbon-like compounds (Aiken et al., 2009). However, in contrast to the typical hydrocarbon-like OA factor characterised by a relatively low OS_C (-1.7 to -1.6, Kroll et al., 2011), the flaming-BBOA contains more oxygen-containing functional groups, and is similar to the primary biomass burning OA factor measured in the RWC exhaust in

a chamber (Tiitta et al., 2016; θ = 13.6°, R^2 = 0.95). Pyrolysis-BBOA, on the other hand, consisted of ions typical to the low-temperature pyrolysis products of wood combustion and correlated well with the PACs (R^2 = 0.86, Fig. ~~S18~~S19).

Of the more-oxygenated factors, the LV-OOA was dominated by the CO^+ and CO_2^+ ions and thus represented highly oxidised OA. The LV-OOA spectra corresponded well with the OH-induced SOA factor identified from the RWC exhaust aged in a smog chamber (Tiitta et al., 2016., θ = 8.4°, R^2= 0.98), and was comparable with that of ambient LV-OOA (Aiken et al., 2009) and the LV-OOA spectra of unaged wood combustion exhaust (Kortelainen et al., 2018). LV-OOA was also present in the unaged exhaust of this study, excluding the dry spruce combustion in the masonry heater, which produced the least-oxidised primary exhaust. The SV-OOA, on the other hand, was related to the $C_2H_3O^+$-ion (R^2 = 0.78), which is indicative of carbonyl formation in the particulate OA (Ng et al., 2010). The SV-OOA was also comparable (θ = 11.5 °, R^2 = 0.96) to a factor of SOA generated in a chamber in the previous work (Tiitta et al., 2016~~)~~), where this factor was~~-~~ interpreted as ozonolysis-generated organic OA. Interestingly, SV-OOA was formed only during photochemical aging and increased in line with higher exposures despite semi-volatile compounds being products of the initial stages of OA oxidation. This further demonstrates the long-continuing functionalisation of OA during aging alongside with the fragmentation processes.

3.5.3 Polycyclic aromatic compounds

PACs were overall more prominent in the primary exhaust of dry spruce combustion (3.2 % of total OA, Fig. ~~1~~19) than ~~in~~from combustion of moist spruce (1.7 % or 2.0 %) or beech (1.7 %). As expected, the total PAC concentrations decreased because of aging and contributed less than 0.5 % to OA for all cases after 3 eqv.d of aging. Furthermore, aging transformed the composition of the PACs assessed with the SP-HR-ToF-AMS HR-PAH analysis (P-~~MPIP~~MIP analysis, Chapter S5.2; Herring et al., 2015). While UnSubPAHs formed the most prominent PAC group of all the combustion experiments, aging decreased their share from 60 % in unaged exhaust to 40–50 % after 3 eqv.d of aging. Similarly to the PACs measured with SP-HR-ToF-AMS, aging decreased the UnSubPAHs analysed with IDTD-GC-ToFMS by 83–85 % in the dry spruce combustion in the masonry heater, and by 90–98 % in the other situations. Of the most prominent UnSubPAHs, anthracene and fluoranthene degraded within the first eqv.d (Fig. ~~1~~210). Also benzo[a]pyrene, which is a used as the marker for total ambient PAHs (EC 2004), degraded by a factor of 5 ~~because of~~as a result of photochemical aging (Table S12).

The ~~decrease~~change in ~~total PAC concentration likely diminished~~ the ~~adverse~~PACs also alters the potential health effects of the exhaust~~; however, there was a~~: although the total PAC concentration decayed, the simultaneous formation of oxy- and nitro-PAC derivatives known to be detrimental to health was observed. These substituted PACs have lower vapour pressures compared to those of parent PAHs and thus are more likely to condense on the particles (Shen et al., 2012). The share of oxygenated PACs ~~(OPAHs)~~ to the total HR-PAH concentration measured by SP-HR-ToF-AMS increased from 15–19 % in unaged exhaust to 25–38 % in aged exhaust. The concentrations of both the SP-HR-ToF-AMS HR-OPAH and IDTD-GC-ToFMS derived OH-PAH also correlated with the SV-OOA PMF factor (Pearson r = 0.70 for OPAH and r = 0.88 for OH-PAH; see Table S11) pointing towards their continuous formation during aging. Of the compounds measured by IDTD-GC-ToFMS, the most notable increase was observed for naphthaldehydic acid, with high concentrations in aged aerosol (up to 100 µg m^{-3}~~)~~ in ~~aged aerosol.~~dilution corrected flue gas). Interestingly, its concentration was highest at approximately 1 eqv.d, after which it decreased. Naphthaldehydic acid and other oxygenated ~~PAHs~~PACs have also been previously found to form during photochemical aging of RWC exhaust (Bruns et al., ~~2015~~2015b; Miersch et al., 2019); however, we found that the photochemically enhanced naphthaldehydic acid

concentration degraded after continuous aging, although remaining considerably higher than ~~those~~ in the unaged emissions.

In addition, the share of nitrogen-substituted ~~PAHs~~PACs, including both NPAH and APAH, increased from a combined share of 5 % of HR-PAH_{tot} (measured by SP-HR-ToF-AMS) in fresh exhaust to a maximum of 9 % in the aged exhaust. In general, particulate nitrogen-substituted ~~PAHs~~PACs are formed in the atmosphere through the oxidation of gaseous PACs or via heterogenous reactions from UnSubPAHs and are also simultaneously degraded by photochemical reactions (Keyte et al., 2013). As UnSubPAHs in the present study were largely consumed after 3 eqv.d, the higher photochemical exposure times consequently led to ~~a decrease in~~situation where the precursors for nitrogen-substituted ~~PAHs~~PACs are not available and therefore no further formation took place.

3.5.4 Organic acids

Photochemical aging led to a considerable increase in particulate organic acids in exhaust aerosol~~.~~ analysed with IDTD-GC-ToF-MS. The amount of small multifunctional acids such as malic acid ($C_4H_4O_4$) and tartaric acid ($C_4H_6O_6$) increased by factors up to greater than 200 (Fig. ~~12~~10, Table S12). Increases in the amounts of also dicarboxylic acids such as succinic ($C_4H_6O_4$) and glutaric acid ($C_5H_8O_4$) were evident, although to a lesser factor. ~~Compared to~~The comparison of IDTD-GC-ToF-MS measurements with the SP-HR-ToF-AMS measurements~~,~~ revealed that the concentrations of organic acids were connected to both LV- and SV-OOA factors ($r > 0.7$, Table S11), which also strongly increased during the aging process. This was expected based on the association of SV-OOA with the $C_2H_3O^+$-ion indicating carbonyl formation. In the n_C-OS_C space (Fig. ~~9~~7), these compounds dominated the upper-right corner with the highest oxidation states and largest enhancement ratios and are close to the LV-OOA region specified for atmospheric OA by Kroll et al. (2011). ~~These~~The measured organic acids were mostly intermediately volatile products of the continuous fragmentation process and partitioned also to the gaseous phase where they ~~in turn participated~~are expected to participate in secondary gas-phase OH reactions. ~~Their~~Overall, the concentrations of particulate organic acids were highest at approximately 3 eqv.d, after which they were degraded by further oxidation reactions.

3.5.5 Nitrophenols

An increase in nitrophenols in the particulate phase was evident during photochemical aging, which increased the concentrations of 4-nitrophenol (4-NP) and 4-nitrocatechol (4-NC) by respective factors of 2–30 and 30–3000 compared to non-aged exhaust (Fig. ~~14).~~10, Table S12) as measured by IDTD-GC-ToFMS. The highest attained 4-NC concentration corresponded to 2 % of total SP-HR-ToF-AMS-based OA concentration, which is a notable fraction for a single compound in an aging aerosol. These secondary nitrophenols were products of OH + phenolic-compound reactions and may have originated from both the gas-phase and heterogenous reactions (Harrison et al., 2005). ~~However,~~Also the ozonolysis ~~in the presence of NO_2~~experiments led to an extensive formation of 4-NP, whereas the amount of 4-NC did not increase. This discrepancy might be the result of absence of the photochemical production of catechol, which is the precursor for 4-NC formation (Finewax et al., 2018).

Nitrophenol concentrations were highest at relatively low OH exposures (1–2 eqv.d) and decreased with increased aging. Similar trends with OH exposure were seen in the NPAH and APAH concentrations measured with SP-HR-ToF-AMS. Nitrophenols are reactive towards OH and photolysis in both gaseous and particulate phases, and ~~as~~ their amount decreased from both phases after the first equivalent days of aging~~, it can be concluded that they overall diminished from~~. Thus, the ~~exhaust with~~measured nitrophenols decay efficiently under high OH-exposures, and therefore

are not ideal biomass combustion markers for long-~~term aging. However~~range transported smoke. On the hand, their concentrations ~~did remain~~still remained higher in the highly aged exhaust than in the fresh exhaust. Furthermore, in the particulate phase, they likely contributed to the formation of organic acids which are formed during the continuous photo-oxidation of the nitrophenols (Hems and Abbatt, 2018).

4 Conclusions

The photochemical aging of dynamically changing OA emitted from RWC was evaluated using the PEAR ~~oxidation flow reactor~~OFR to expose the exhaust to varying photochemical conditions for up to an equivalent of one week in the atmosphere. To evaluate typical Northern and Central European combustion emissions, two different appliances were used with regionally typical logwood fuels. While the primary concentrations of particulate OA were relatively similar for all of the assessed sources, the enhancement of the organic particulate carbon during aging depended on the type of the fuel. In particular, the fuel moisture content affected the SOA production ~~with~~: dry fuel ~~producing~~produced a ~~smaller~~lower organic mass and OA enhancement during aging than moist wood, because ~~the OA enhancement was strongly influenced by the~~ of the significantly lower emission rates of the organic gases~~, which were significantly lower for dry spruce.~~. However, a very low (5 %) logwood moisture content ~~also~~ considerably increased the primary PM_1 emission because of the extensive soot formation. With current logwood combustion appliances, this presents a conflict in ~~emission reduction intended to decrease the different constituents in RWC exhaust with overly dry logwood producing large black carbon emissions and moist fuel increasing oxygenated emissions.~~attempts to decrease emissions since the usually preferred dry logwood produces high BC emissions while high moisture content of the fuel increases the amount of organic emissions, as shown here for spruce logwood. Similar phenomenon has, however, been recently noted also for hardwood fuels (Tissari et al., 2019).

The particulate organic carbon mass in the RWC exhaust increased by a factor of 1.3–3.9 during photochemical aging. Furthermore, photochemical aging transformed the overall composition of the OAs. This was observed as a linear increase in the average carbon oxidation state of particulate OA throughout the investigated photochemical exposure range, while the ratio of organic carbon to total organic mass decreased. Photochemical aging caused multiform changes in the OA also at the molecular level. Notably, small~~,~~ acidic reaction and fragmentation products became increasingly dominant in both particulate and gaseous phases with higher aging. The concentrations of particulate nitrophenols were at their highest level after 1 eqv.d, after which they began to ~~decaying~~decay but remained higher than that in the primary exhaust. Similarly, nitrogen-containing aromatics were unobservable in the gaseous phase at longer exposures, although they have been observed to increase during exposures less than 1 eqv.d (Hartikainen et al., 2018). Aging also enhanced the share of oxygen- and nitrogen-substituted polycyclic aromatic compounds in the PAC emissions. Of the oxygenated PACs, naphthaldehydic acid in particular increased considerably with concentrations peaking at approximately 1 eqv.d. However, PACs in total degraded almost completely after 3 eqv.d of aging.

~~Based on this work,~~ In general, several different oxidation mechanisms of organic aerosol are likely occurring simultaneously both in the atmosphere and in the OFR experiments of this study. However, based on the observed OA chemical compositions under a range of different OH-exposures, different major transformation ~~pathways~~mechanisms for RWC exhaust under photochemical conditions can be roughly outlined~~: the initial pathways consisting of functionalisation and~~. First, the results demonstrate that short OH-exposures (~1 eqv.d) are sufficient to functionalize the majority of gaseous SOA precursors of RWC exhaust and lead to their condensation ~~from gaseous precursors are followed by more~~into particulate- phase~~-driven chemistry consisting of~~. This mechanism dominates the overall OA transformation

until the SOA precursors have been depleted. After this stage, the continuing OH-exposure leads to further oxidation of particulate organic aerosol, which is likely explained by heterogeneous ~~oxidation and fragmentation.~~ reactions between gas-phase oxidants and particles. However, it is also possible that particulate phase oxidation occurs via evaporation and homogeneous gas-phase oxidation followed by recondensation.

While several recent studies (Bertrand et al., 2017; Bruns et al., ~~2015~~2015b; Bruns et al., 2017; Grieshop et al., 2009; Hartikainen et al., 2018; Heringa et al., 2011; Pieber et al., 2018; Tiitta et al., 2016) have assessed the behaviour of RWC emissions in a relatively short timescale of less than ~~1.5~~2 eqv.d, ~~the results of~~ this study ~~emphasise~~highlights the importance of ~~investigating longer photochemical exposures. This is particularly relevant considering~~also higher exposure levels towards chemical transformation of OA. Due to the potentially long atmospheric lifetimes of OA ~~and its importance~~, long-term aging is also important to consider in large-scale atmospheric models, which typically estimate SOA formation and characteristics based on short-term ~~chamber experiments. Atmospheric OA is a mixture of emissions from various sources having diverse exposure levels from fresh emissions to~~ aging experiments. The consideration of only the first stage of gas-phase functionalization and condensation may lead to underestimated oxygenation of the long-transported ~~highly oxidised OAs. The~~OA, while specific compound groups, such as nitrophenols or substituted-PACs, can be overestimated. In general, the potential health and climate effects of aerosols are to a large extent determined by their composition, which depends on their sources and the levels of atmospheric aging. Thus, the characterisation of aerosol emissions from different sources and their atmospheric transformation at different exposure levels ~~is~~would be crucial ~~when assessing~~for assessment of the overall environmental effects of ambient air pollution.

Table 1: Combustion conditions and experimental conditions of each experiment.

	Exp.	hv flux [photons cm^{-2} s^{-1}]	O_3 ~~input~~ [ppm]	Initial age* [eqv. d]	Fuel	OH exp. [# s cm^{-3}]	Age [eqv.d]	MCE	~~VOC~~OGC/NO_x	DR
Masonry heater	1	lamps off	0	no-OH	S-5%			0.979	1.5	64
					S-22%			0.974	4.9	83
	2	8.~~3E~~6E+15	2.3	14.07	S-5%	5.8E+11	6.~~7~~8	0.975	1.2	137
					S-22%	3.5E+11	4.0	0.978	3.1	147
	3	lamps off	2.5	no-OH	S-5%			0.974	1.3	135
					S-22%			0.973	4.0	144
	4	~~1.9E~~2.8E+15	2.2	5.84	S-5%	1.5E+11	1.7	0.974	1.4	130
					S-22%	1.3E+11	1.5	0.966	5.5	152
	5	1.4E+15	1.8	2.35	S-5%	8.1E+10	0.9	0.971	1.3	160
					S-22%	6.3E+10	0.7	0.976	3.7	196
Chimney stove	1	lamps off	0	no-OH	B-17%			0.968	1.6	72
					S-22%			0.966	5.4	80
	2	5.~~4E~~8E+15	4.3	12.90	B-17%	3.1E+11	3.6	0.963	1.8	122
					S-22%	not meas.	~4**	0.965	3.6	148
	3	lamps off	3.1	no-OH	B-17%			0.953	1.9	124
					S-22%			0.961	4.9	143
	4	1.1E+15	3.6	5.10	B-17%	5.4E+10	0.6	0.951	1.7	119
					S-22%	6.1E+10	0.7	0.972	4.2	135
	5	1.1E+16	11	18.76	B-17%	5.0E+11	5.8	0.962	1.5	36
					S-22%	5.0E+11	5.8	0.957	5.6	40

*Age based on the OH-exposure of clean air, prior to sample input.
** Direct OH exposure measurements not available for Chimney stove Exp. 2 S-22%; approximately similar as in Exp. 2 B-17%.

Table 2: Primary PM_1 ~~emissions~~concentrations in dry ~~13% O_2 exhaust~~flue gas. The number concentration and geometric mean mobility diameter (GMD) were derived from a scanning mobility particle sizer and PM1, organic carbon, and elemental carbon from filter samples.

	Number ~~([~~10^7 # cm^{-3}~~)]~~	GMD ~~([~~nm~~)]~~	PM_1 ~~([~~mg m^{-3}~~)]~~	OC ~~([~~mg m^{-3}~~)]~~	EC ~~([~~mg m^{-3}~~)]~~	OC:EC
Masonry heater, spruce 5 % H_2O (S-5%)	3.2 ± 0.6	95.5 ± 24.4	67 ± 16	4.3 ± 1.9	57.1 ± 15.8	0.07 ± 0.02
Masonry heater, spruce 22 % H_2O (S-22%)	4.5 ± 1.6	68.4 ± 22.2	33 ± 16	4.4 ± 4.6	19.1 ± 12	0.31 ± 0.45
Chimney stove, beech 17 % H_2O (B-17%)	4.4 ± 0.4	61.1 ± 7.6	43 ± 11	3.0 ± 1.4	21.9 ± 11.1	0.15 ± 0.04
B-17% : 1^{st} to 2^{nd} batch	4.3 ± 1.9	71.6 ± 5.7	48 ± 4	4.2 ± 0.9	32.0 ± 5.3	0.12 ± 0.01
B-17% : 3^{rd} to 4^{th} batch	5.4 ± 0.9	57.2 ± 5	38 ± 13	1.9 ± 0.6	11.8 ± 3.3	0.18 ± 0.03
Chimney stove, spruce 22 % H_2O (S-22%)	4.5 ± 0.3	52.8 ± 13.3	37 ± 8	4.3 ± 0.7	17.0 ± 2.0	0.25 ± 0.04

Table 3: Properties of the PMF factors.

Factor	*O:C*	*H:C*	*N:C*	*OSc*	*OM:OC*
LV-OOA	1.57	0.97	5.97E-03	2.18	3.19
SV-OOA	0.78	1.41	1.78E-03	0.16	2.17
Flaming-BBOA	0.55	1.52	4.33E-03	-0.42	1.86
Pyrolysis-BBOA	0.49	1.41	2.13E-03	-0.44	1.77

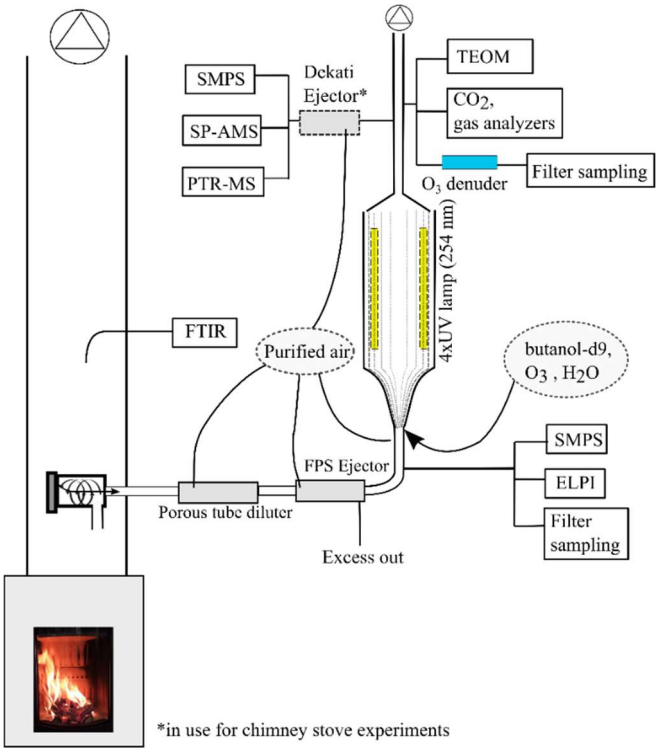

Figure 1: Experimental setup.

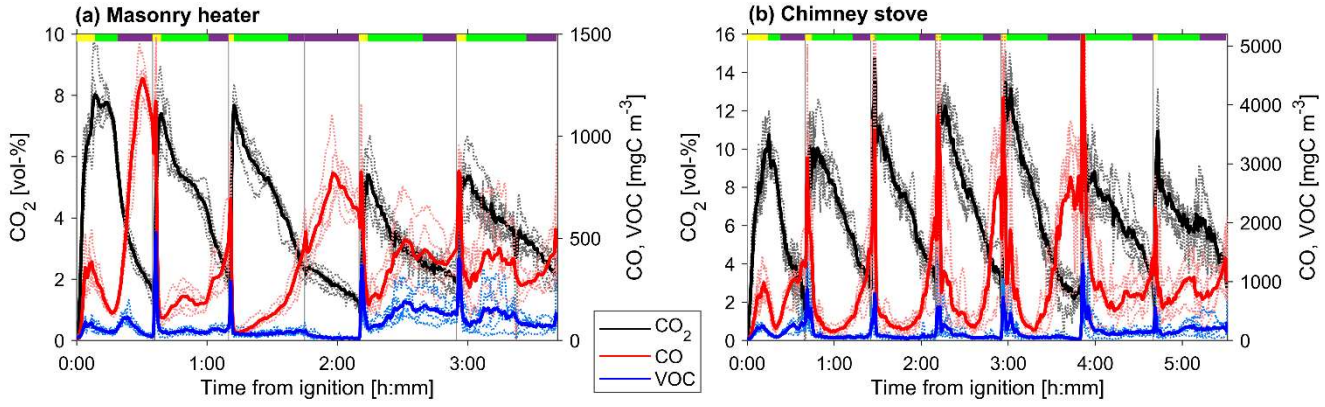

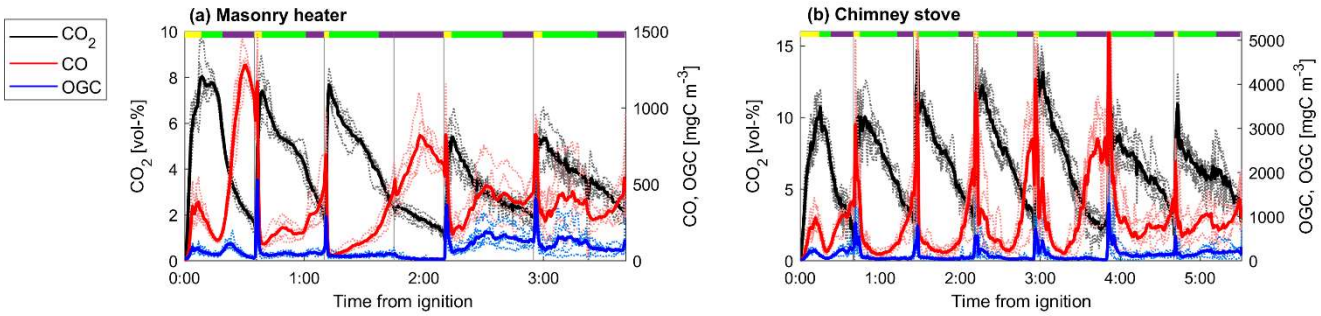

Figure 2: CO_2, and CO, and the ~~VOCs~~OGC in the dry exhaust gas from (a) masonry heater, and (b) chimney stove, measured by FTIR. Averages over all experiments are shown with solid lines, whereas different experiments are shown with dotted lines. Average phase lengths are marked on the top panel with the yellow (ignition), green (flaming), and purple (burnout).

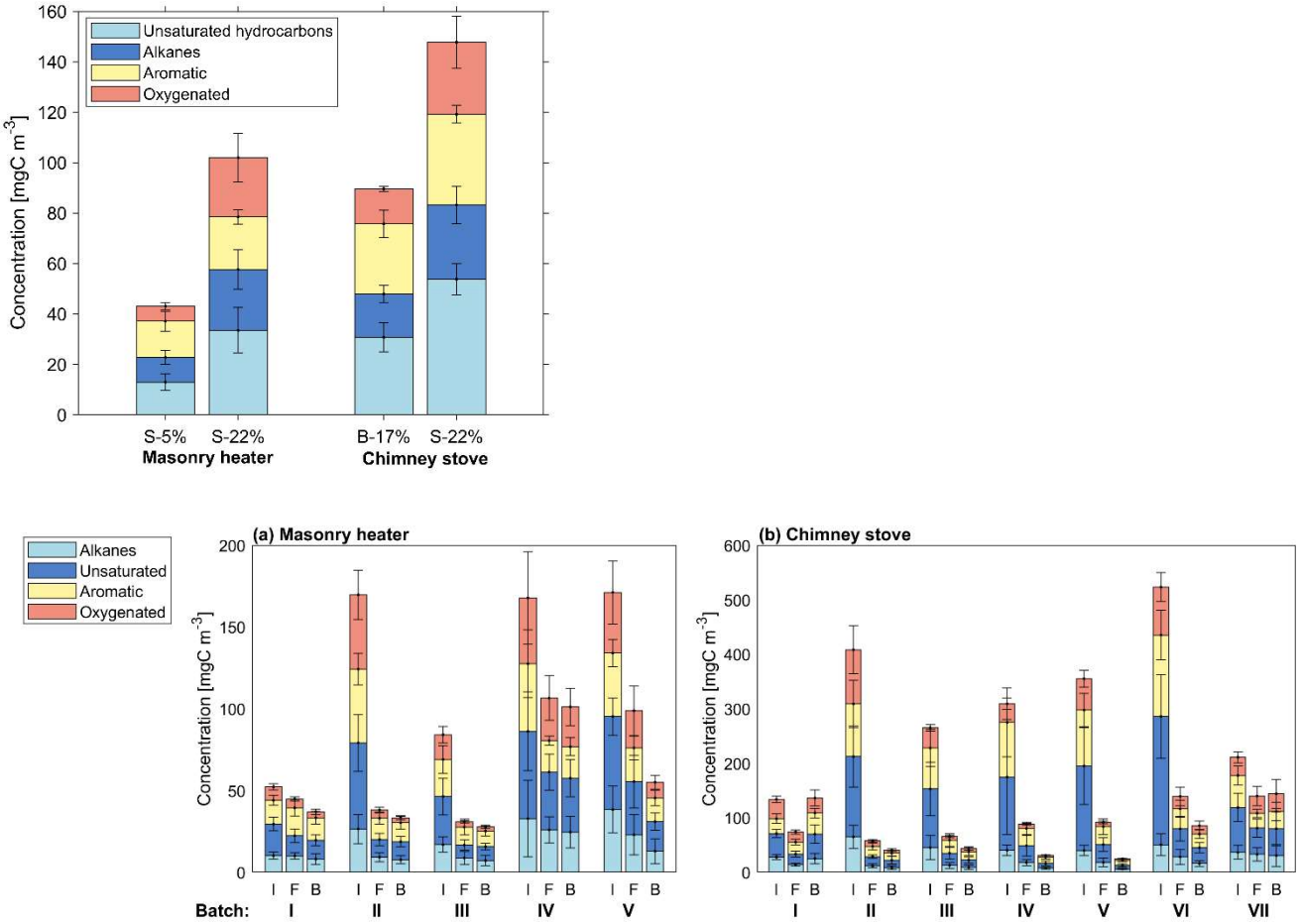

Figure 3: Average concentrations of organic gaseous compounds in the dry primary exhaust at the different combustion phases (I=ignition, F=flaming, B=char burnout phase) for each batch measured by FTIR from the stack. Error bars denote standard deviations between experiments.

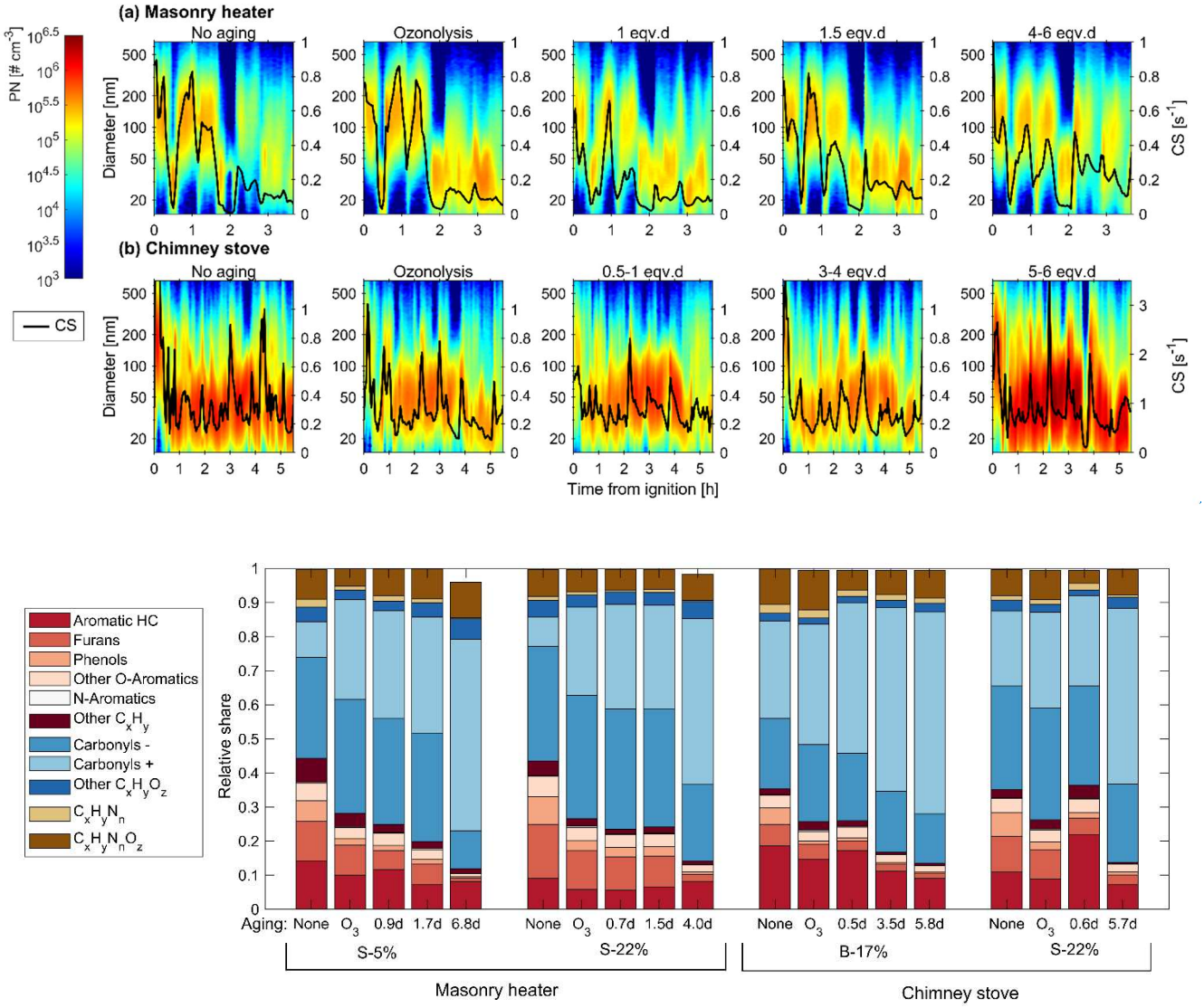

Figure 4: ~~Size distributions of diluted primary aerosol entering the oxidation flow reactor as a function of time, and condensation sinks (CS) in the PEAR based on average of size distributions before and after PEAR.~~

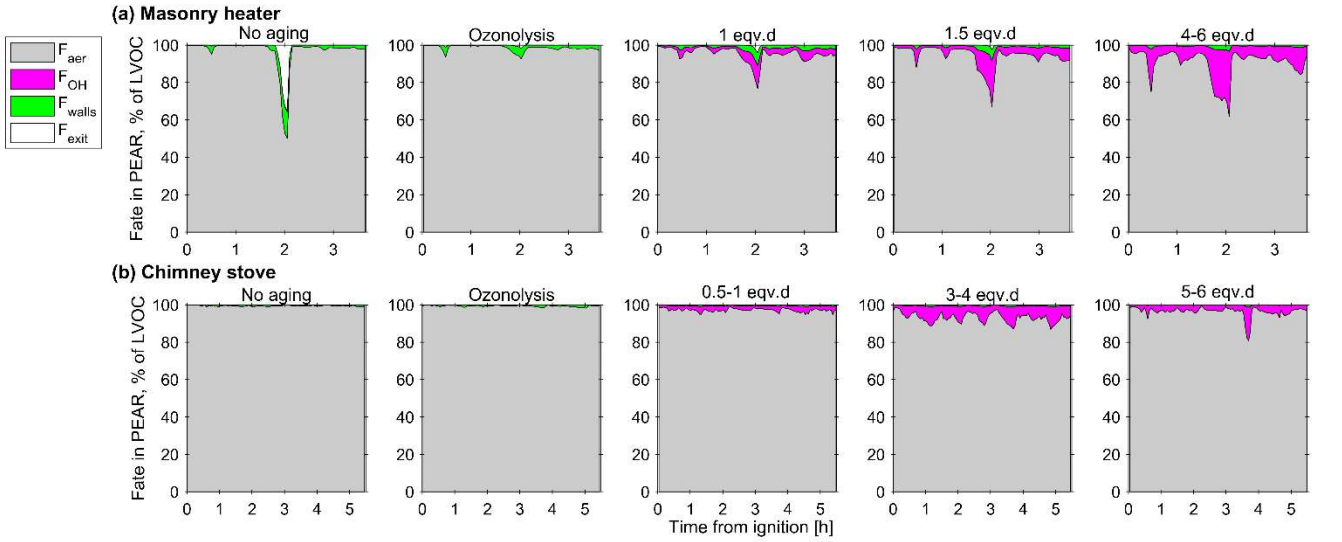

~~Figure 5: Estimated fates of the low-volatility organic compounds in the PEAR during the experiments with portions of the LVOCs condensing onto particles (F_{aer}) and walls (F_{walls}) and lost in reactions with OH (F_{OH}). The remainder of the LVOCs (F_{exit}) exit the PEAR as LVOCs.~~

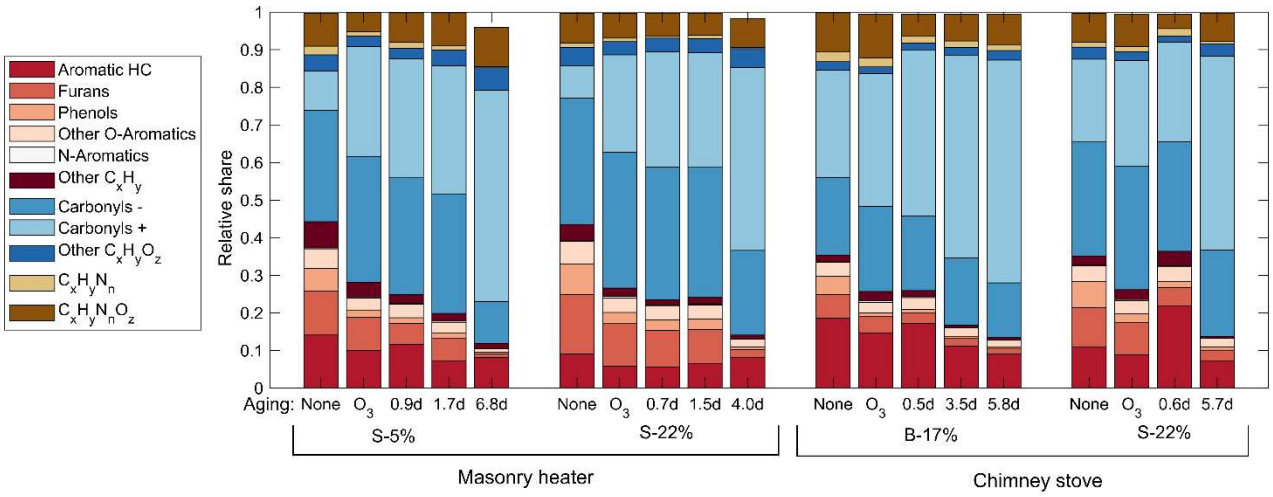

~~Figure 6:~~ Relative shares of the ~~identified VOC~~OGC groups in the exhaust ~~after~~downstream the PEAR OFR as measured by PTR-ToF-MS, averaged over the total experiment time covering 2–5 batches.

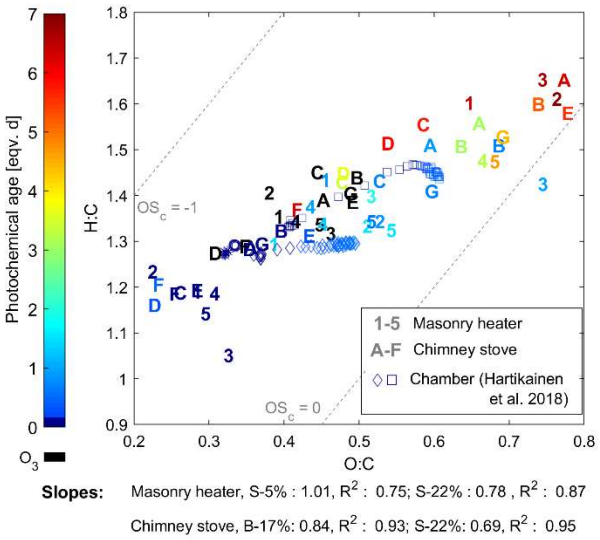

Slopes: Masonry heater, S-5% : 1.01, R^2 : 0.75; S-22% : 0.78 , R^2 : 0.87

Chimney stove, B-17%: 0.84, R^2 : 0.93; S-22%: 0.69, R^2 : 0.95

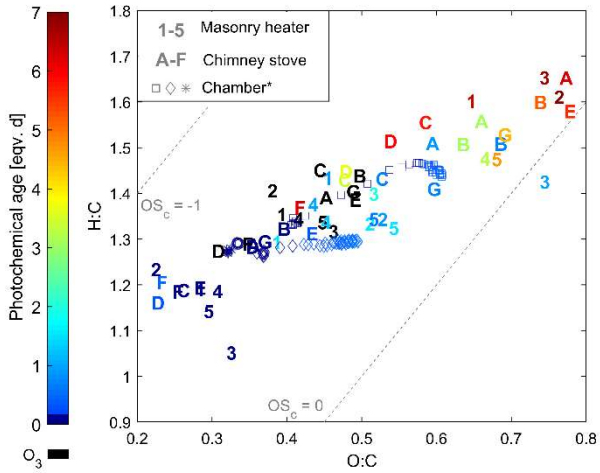

Slopes: Masonry heater, S-5% : 1.01, R^2 : 0.75; S-22% : 0.78 , R^2 : 0.87

Chimney stove, B-17%: 0.84, R^2 : 0.93; S-22%: 0.69, R^2 : 0.95

Figure ~~7~~5: Van Krevelen diagram of the ~~VOCs~~OGCs measured ~~with~~by PTR-ToF-MS. Numbers indicate batches combusted in masonry heater (1–3 dry spruce, 4–5 moist spruce); letters refer to chimney stove batches (A–E beech, F–G moist spruce). Ozonolysis experiments (in black) were not considered in the slope calculations. *Behaviour of RWC emission aged in a chamber (Hartikainen et al., 2018) ~~is marked with scatter.~~

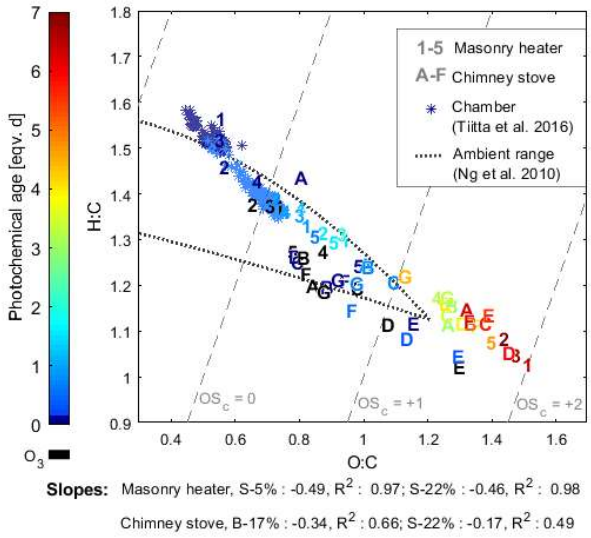

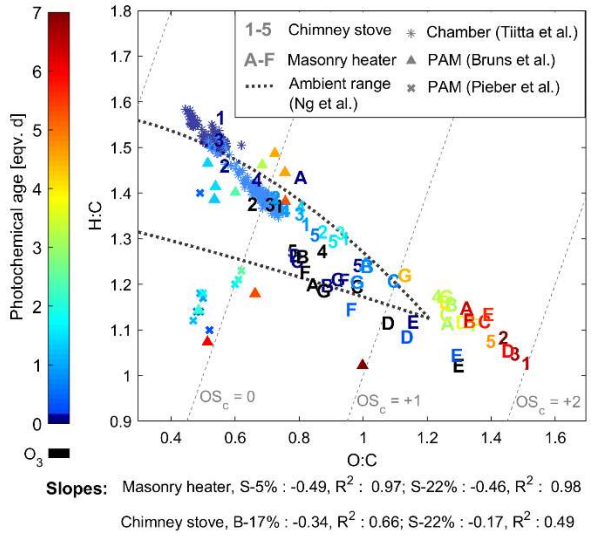

Figure ~~8~~6: Van Krevelen diagram of the particulate organic aerosol measured by SP-HR-ToF-AMS. Numbers indicate batches combusted in masonry heater (1–3 dry spruce, 4–5 moist spruce), whereas letters refer to chimney stove batches (A–E beech, F–G moist spruce~~).~~) of this study. Ozonolysis experiments are marked with black and were not considered in slope calculations. ~~The~~Results from aging of RWC exhaust with a PAM OFR by Bruns et al. (2015a) and Pieber et al. (2018), as well as behaviour of RWC OA aged in a chamber (Tiitta et al., 2016) ~~with slopes of -0.64 to -0.67 is~~are marked with scatter.

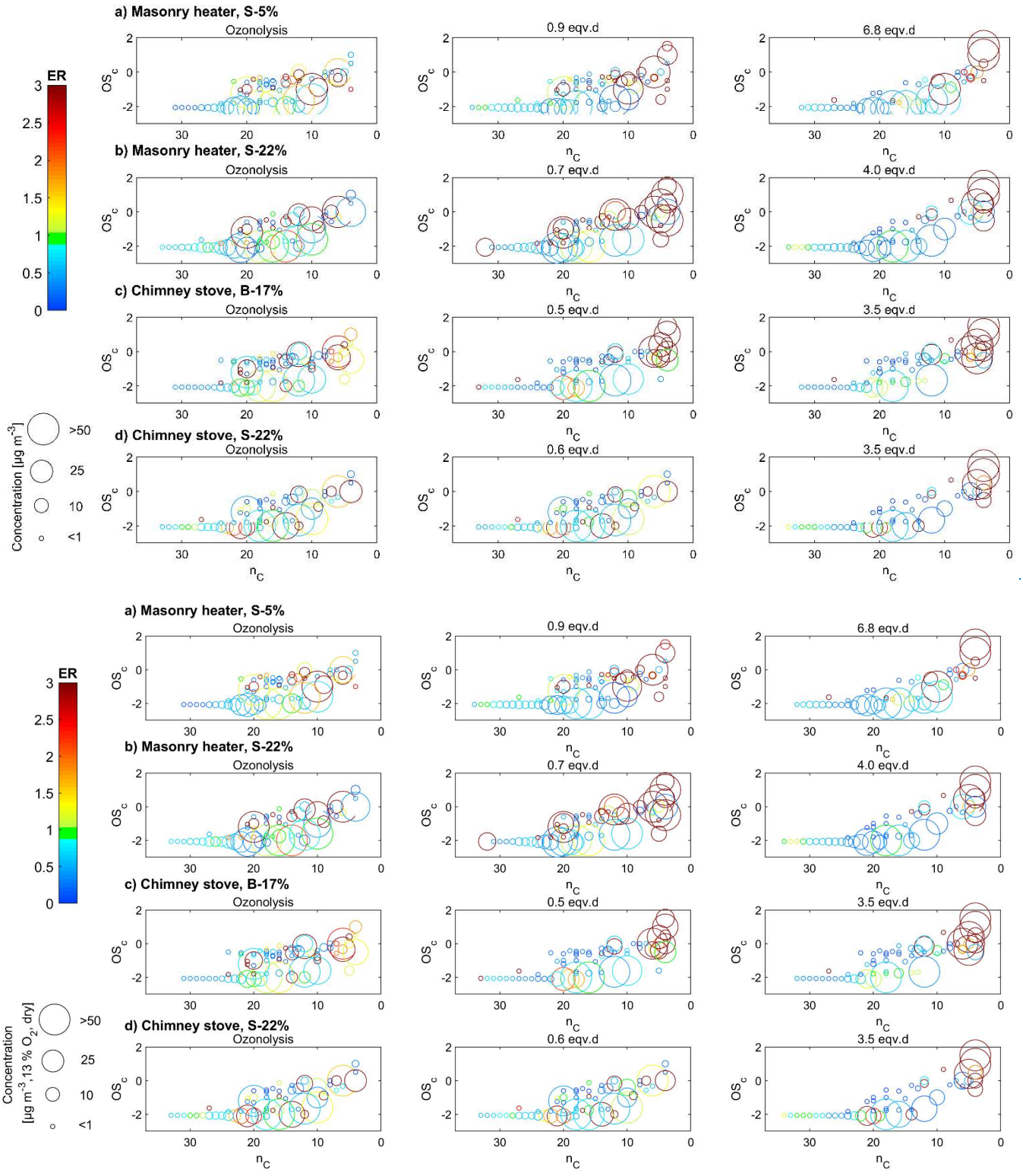

Figure 97: Compounds measured by IDTD-GC-ToFMS in different experiments (ozonolysis, low, and high photochemical exposure) with respect to their carbon number (n_C) and oxidation state (OS_C). Enhancement ratios (ER) compared to the experiments without oxidative aging are shown in colour, and the size indicates the dilution-corrected concentrations (normalised dry, 13% O_2 flue gas conditions) in the secondary exhaust.

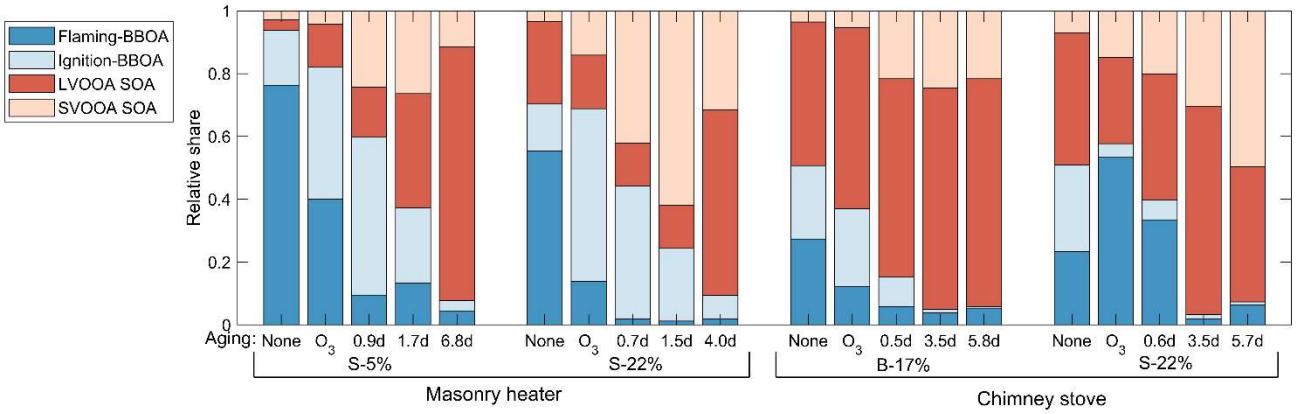

Figure ~~10~~8: Average shares of the four PMF factors in the exhaust ~~after the PEAR at the~~at different exposure levels.

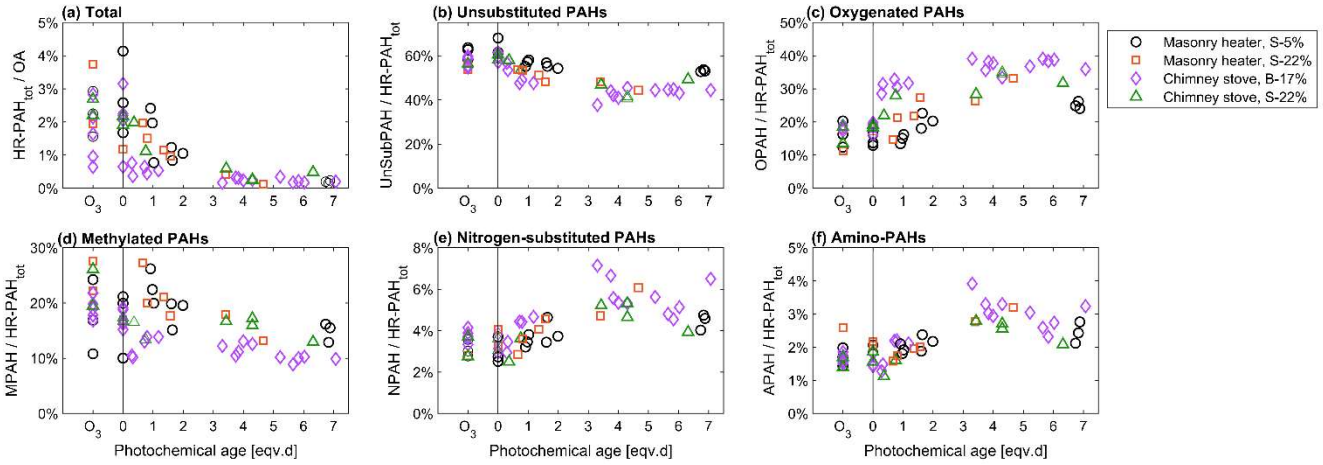

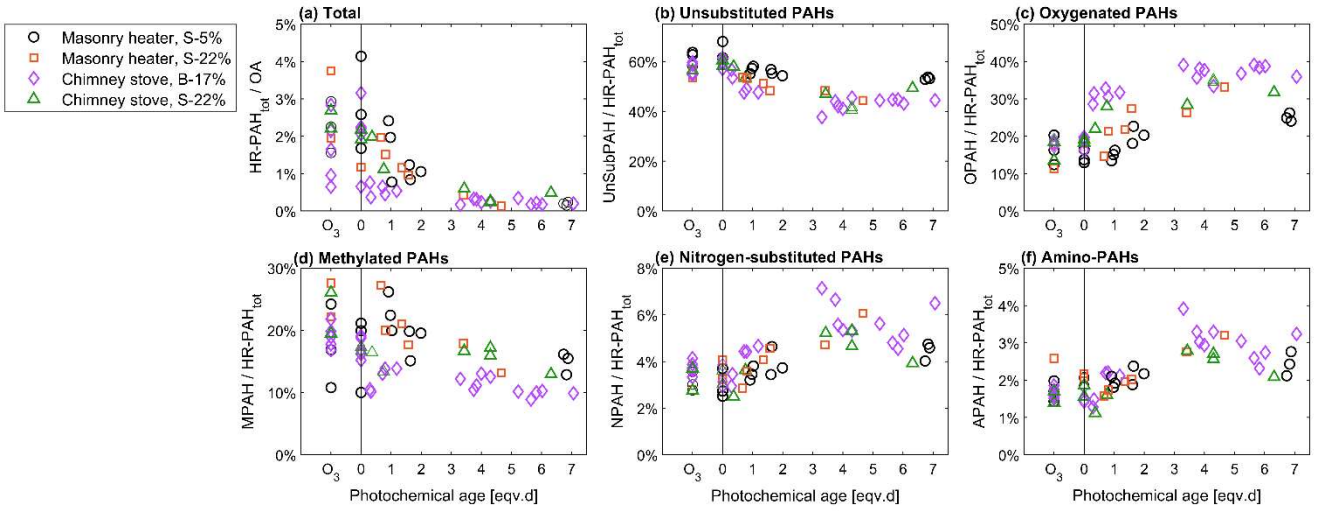

Figure ~~11~~9: Relationship of photochemical aging to the batchwise average ratios of~~:~~ (a) total HR-PAH concentration to OA concentration ~~measured by AMS,~~ and (b–f) of HR-PAH subgroups to the total PAC concentration, measured by the SP-HR-ToF-AMS.

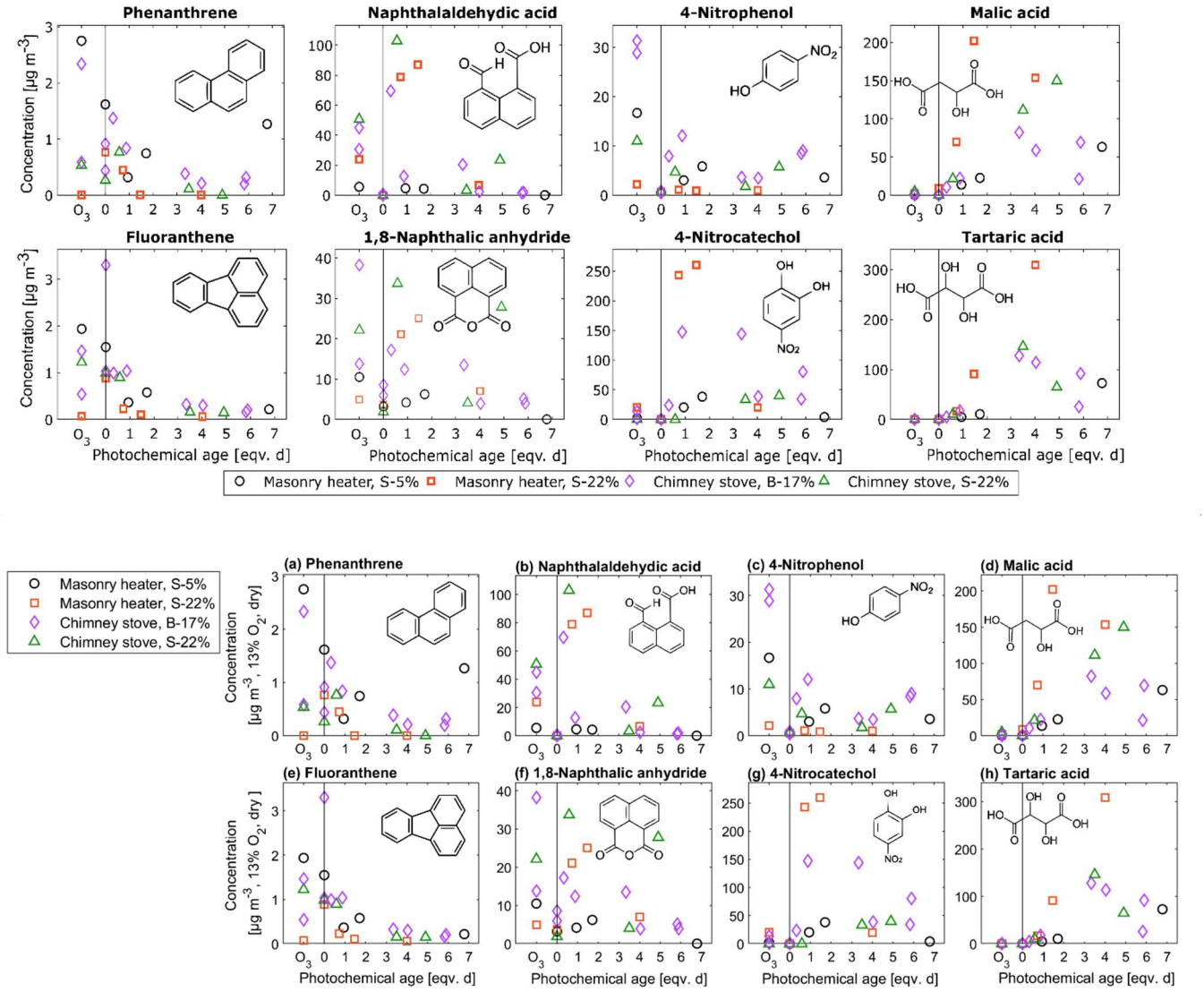

Figure ~~12: Concentrations of~~10: Dilution corrected concentrations for selected compounds measured by IDTD-GC-ToFMS at different exposure levels. Normalised to dry, 13% O_2 flue gas conditions.